We are IntechOpen,
the world's leading publisher of
Open Access books
Built by scientists, for scientists

7,000
Open access books available

187,000
International authors and editors

205M
Downloads

154
Countries delivered to

Our authors are among the

TOP 1%
most cited scientists

12.2%
Contributors from top 500 universities

BOOK CITATION INDEX
CLARIVATE ANALYTICS
INDEXED

WEB OF SCIENCE™

Selection of our books indexed in the Book Citation Index
in Web of Science™ Core Collection (BKCI)

Interested in publishing with us?
Contact book.department@intechopen.com

Numbers displayed above are based on latest data collected.
For more information visit www.intechopen.com

Switched Reluctance Motor

Jin-Woo Ahn, Ph.D
Kyungsung University
Korea

1. Introduction

Switched Reluctance Motors (SRM) have inherent advantages such as simple structure with non winding construction in rotor side, fail safe because of its characteristic which has a high tolerances, robustness, low cost with no permanent magnet in the structure, and possible operation in high temperatures or in intense temperature variations. The torque production in switched reluctance motor comes from the tendency of the rotor poles to align with the excited stator poles. The operation principle is based on the difference in magnetic reluctance for magnetic field lines between aligned and unaligned rotor position when a stator coil is excited, the rotor experiences a force which will pull the rotor to the aligned position. However, because SRM construction with doubly salient poles and its non-linear magnetic characteristics, the problems of acoustic noise and torque ripple are more severe than these of other traditional motors. The torque ripple is an inherent drawback of switched reluctance motor drives. The causes of the torque ripple include the geometric structure including doubly salient motor, excitation windings concentrated around the stator poles and the working modes which are necessity of magnetic saturation in order to maximize the torque per mass ratio and pulsed magnetic field obtained by feeding successively the different stator windings. The phase current commutation is the main cause of the torque ripple.

The torque ripple can be minimized through magnetic circuit design in a motor design stage or by using torque control techniques. In contrast to rotating field machines, torque control of switched reluctance machines is not based on model reference control theory, such as field-oriented control, but is achieved by setting control variables according to calculated or measured functions. By controlling the torque of the SRM, low torque ripple, noise reduction or even increasing of the efficiency can be achieved. There are many different types of control strategy from simple methods to complicated methods. In this book, motor design factors are not considered and detailed characteristics of each control method are introduced in order to give the advanced knowledge about torque control method in SRM drive.

1.1 Characteristic of Switched Reluctance Motor

The SRM is an electric machine that converts the reluctance torque into mechanical power. In the SRM, both the stator and rotor have a structure of salient-pole, which contributes to produce a high output torque. The torque is produced by the alignment tendency of poles. The rotor will shift to a position where reluctance is to be minimized and thus the inductance of the excited winding is maximized. The SRM has a doubly salient structure,

but there are no windings or permanent magnets on the rotor [Lawrenson, 1980]. The rotor is basically a piece of steel (and laminations) shaped to form salient poles. So it is the only motor type with salient poles in both the rotor and stator. As a result of its inherent simplicity, the SRM promises a reliable and a low-cost variable-speed drive and will undoubtedly take the place of many drives now using the cage induction, PM and DC machines in the short future. The number of poles on the SRM's stator is usually unequal to the number of the rotor to avoid the possibility of the rotor being in a state where it cannot produce initial torque, which occurs when all the rotor poles are aligned with the stator poles. Fig.1 shows a 8/6 SRM with one phase asymmetric inverter. This 4-phase SRM has 8 stator and 6 rotor poles, each phase comprises two coils wound on opposite poles and connected in series or parallel consisting of a number of electrically separated circuit or phases. These phase windings can be excited separately or together depending on the control scheme or converter. Due to the simple motor construction, an SRM requires a simple converter and it is simple to control.
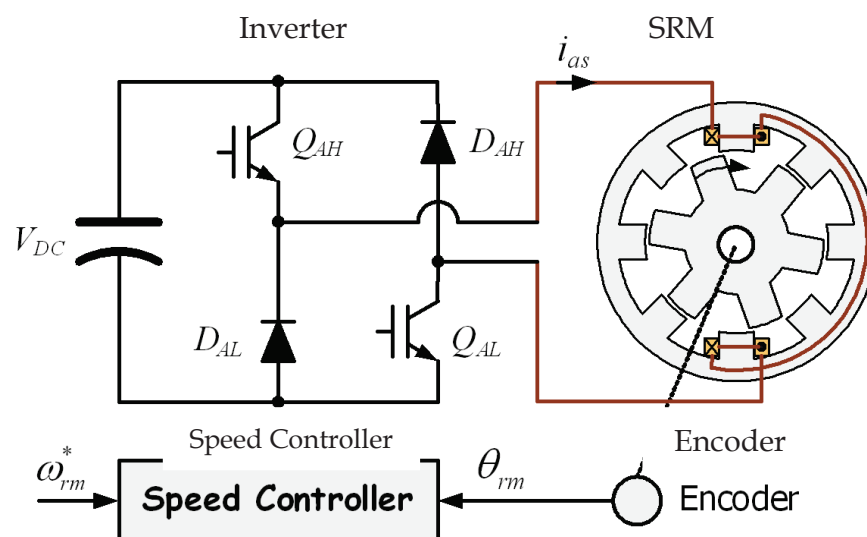

Fig. 1. SRM with one phase asymmetric inverter

The aligned position of a phase is defined to be the situation when the stator and rotor poles of the phase are perfectly aligned with each other ($\theta_1 - \theta_2$), attaining the minimum reluctance position and at this position phase inductance is maximum (L_a). The phase inductance decreases gradually as the rotor poles move away from the aligned position in either direction. When the rotor poles are symmetrically misaligned with the stator poles of a phase ($\theta_3 - \theta_s$), the position is said to be the unaligned position and at this position the phase has minimum inductance (L_u). Although the concept of inductance is not valid for a highly saturated machine like SR motor, the unsaturated aligned and unaligned incremental inductances are the two key reference positions for the controller. The relationship between inductance and torque production according to rotor position is shown in Fig. 2.

There are some advantages of an SRM compared with the other motor type. The SRM has a low rotor inertia and high torque/inertia ratio; the winding losses only appear in the stator because there is no winding in the rotor side; SRM has rigid structure and absence of permanent magnets and rotor windings; SRM can be used in extremely high speed application and the maximum permissible rotor temperature is high, since there are no permanent magnets and rotor windings [Miller, 1988].
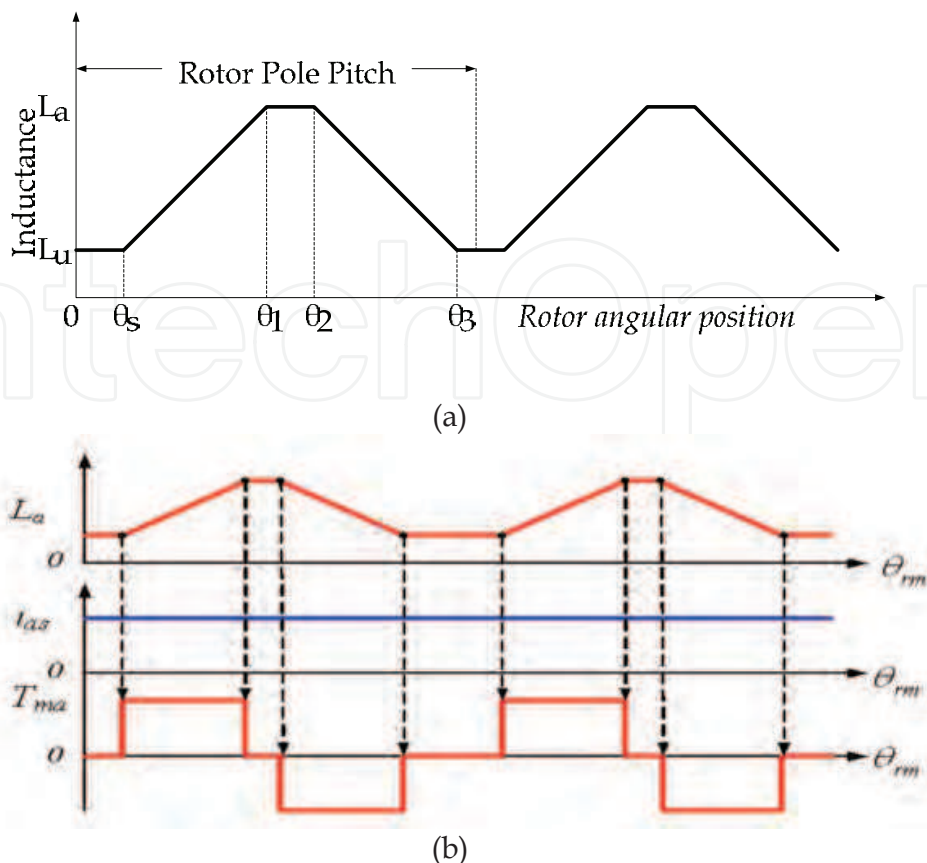
(a)

(b)

Fig. 2. (a) Inductance and (b) torque in SRM

Constructions of SRM with no magnets or windings on the rotor also bring some disadvantage in SRM. Since there is only a single excitation source and because of magnetic saturation, the power density of reluctance motor is lower than PM motor. The construction of SRM is shown in Fig. 3. The dependence on magnetic saturation for torque production, coupled with the effects of fringing fields, and the classical fundamental square wave excitation result in nonlinear control characteristics for the reluctance motor. The double saliency construction and the discrete nature of torque production by the independent phases lead to higher torque ripple compared with other machines. The higher torque ripple, and the need to recover some energy from the magnetic flux, also cause the ripple current in the DC supply to be quite large, necessitating a large filter capacitor. The doubly salient structure of the SRM also causes higher acoustic noise compared with other machines. The main source of acoustic noise is the radial magnetic force induced. So higher torque ripple and acoustic noise are the most critical disadvantages of the SRM.

The absence of permanent magnets imposes the burden of excitation on the stator windings and converter, which increases the converter kVA requirement. Compared with PM brushless machines, the per unit stator copper losses will be higher, reducing the efficiency and torque per ampere. However, the maximum speed at constant power is not limited by the fixed magnet flux as in the PM machine, and, hence, an extended constant power region of operation is possible in SRM.

The torque-speed characteristics of an SRM are shown in Fig. 4. Based on different speed ranges, the motor torque generation has been divided into three different regions: constant torque, constant power and falling power region.
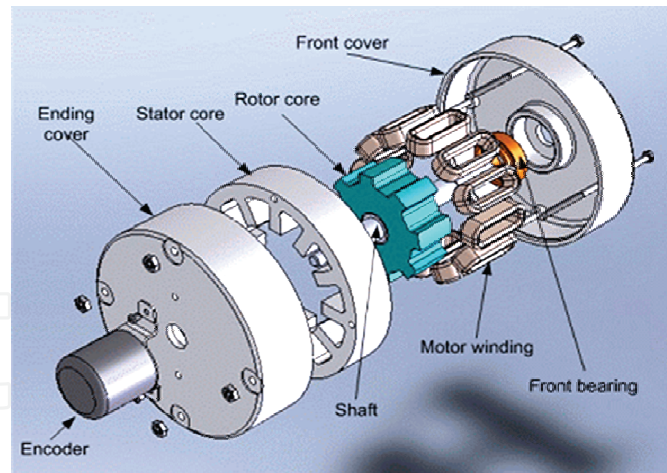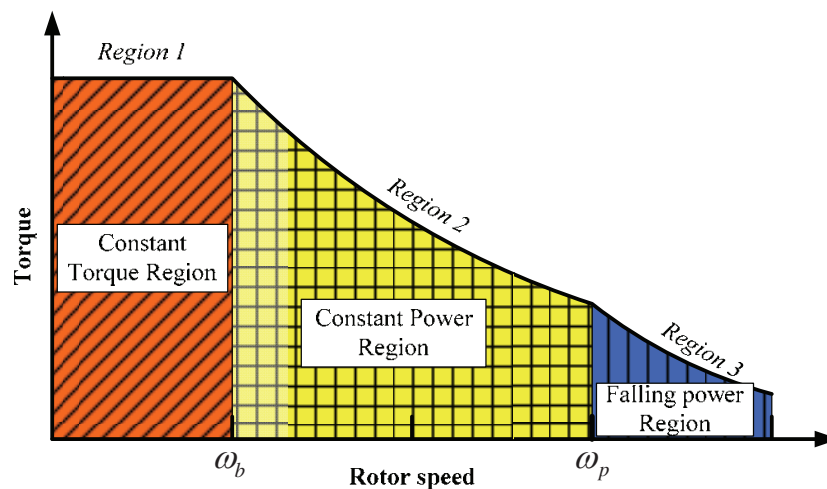
Fig. 3. The construction of SRM

Fig. 4. The torque-speed of SRM

The base speed ω_b is the maximum speed at which maximum current and rated torque can be achieved at rated voltage. Below ω_b, the torque can be maintained constant or control the fat-top phase current. At lower speed, the phase current rises almost instantly after the phase switches turn-on since the back EMF is small at this time. So it can be set at any desired level by means of regulators (hysteresis or PWM controller). Therefore, the adjustment of firing angle and phase current can reduce noise and improve torque ripple or efficiency.

With speed increase, the back-EMF is increased. An advance turn-on angle is necessary to reach the desired current level before rotor and stator poles start to overlap. The desired current level depends on the speed and the load condition. At the same time, since no current chopping appears during the dwell angle, only the angle control can be used at this stage. So the torque cannot be kept constant and is falling linearly with the speed increase, resulting in a constant power production.

In the falling power region, as the speed increases, the turn-on angle cannot be advanced further. Because torque falls off more rapidly, the constant power cannot be maintained. As the speed grows, the tail current of the phase winding extends to the negative torque region.

The tail current may not even drop to zero. In the high speed operation, the continued conduction of current in the phase winding can increase magnitude of phase current and the power density can be increased.

1.2 Equivalent circuit of Switched Reluctance Motor

The equivalent circuit for SRM can be consisting of resistance and inductance with some condition. The effects of magnetic saturation, fringing flux around the pole corners, leakage flux, and the mutual coupling of phases are not considered. The linear analytical model of the SRM can be described by three differential equations, which can be classified as the voltage equation, the motional equation and the electromagnetic torque equation. The voltage equation is:

$$V = R.i + \frac{d\lambda(\theta,i)}{dt} \tag{1}$$

An equivalent circuit of the SRM is shown in Fig. 5. Where V is the applied phase voltage to phase, R is the phase resistance, and e is back-EMF. Ordinarily, e is the function of phase current and rotor position, and λ can be expressed as the product of inductance and winding current:

$$\lambda(\theta,i) = L(\theta,i).i \tag{2}$$

And from (1) and (2), the function can be rewritten as:

$$V = R.i + \frac{d\lambda(\theta,i)}{di} \cdot \frac{di}{dt} + \frac{d\lambda(\theta,i)}{d\theta} \cdot \frac{d\theta}{dt} \tag{3}$$
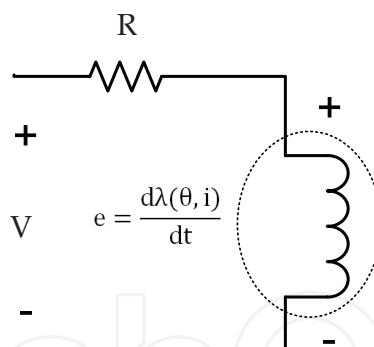

Fig. 5. Equivalent circuit of SR motor

For the electromechanical energy conversion, a nonlinear analysis takes account of the saturation of the magnetic circuit. Generally, the stored magnetic energy is defined as W_f and the co-energy is defined as W_c:

$$W_f = \int i \, d\psi \tag{4}$$

$$W_c = \int \psi \, di \tag{5}$$

The relationship between energy (W_f) and co-energy (W_c) as a function of flux and current shows in Fig. 6.

When rotor position matches the turn-on position, the phase switches are turned on; the phase voltage starts to build up phase current. At this time, one part of the input energy will
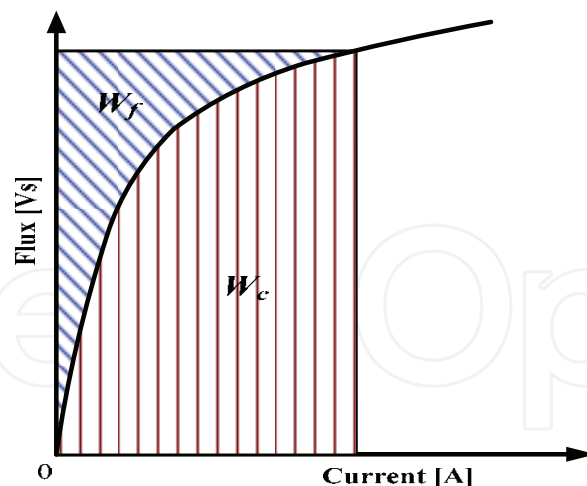
Fig. 6. Relationship between energy (W_f) and co-energy (W_c)

be stored in magnetic field. With the increasing inductance, the magnetic field energy will increase until turn-off angle. The other parts of input energy will be converted to mechanical work and loss. In Fig. 7, the flux of the SR motor operation is not a constant; nevertheless, uniform variation of the flux is the key point to obtain smoothing torque. W_1 is the mechanical work produced during the magnetization process, in other words, W_1 is co-energy in energy conversion. $F+W_2$ is magnetic field energy between turn-on and turn-off. During the derivation of the energy curve and the energy balance, constant supply voltage Vs and rotor speed ω are assumed.

When rotor position matches the turn-off position, phase switches are turned off. So the power source will stop to input energy. But magnetic field energy is $F+W_2$ at that moment. The magnetic field energy needs to be released, and then the phase current starts to feedback energy to power source. At this time, some of magnetic field energy, which is W_2, is converted into mechanical work and loss. The surplus of field energy F is feedback to the power source.
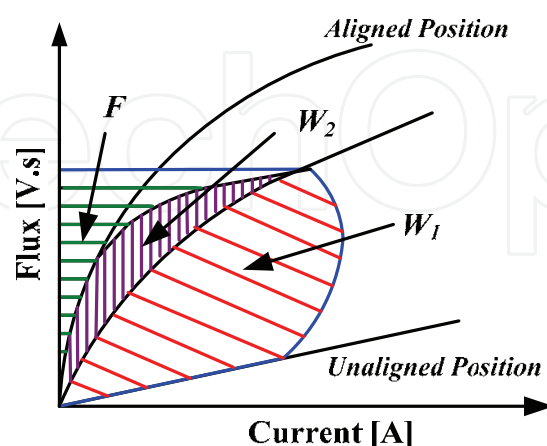

Fig. 7. Graphical interpretation of energy and co-energy for SR motor

The analytical answer of the current can be obtained from (3). The electromagnetic torque equation is:

$$T_e = \frac{\partial W'}{\partial \theta} = \frac{\partial W'(\theta + \Delta\theta) - \partial W'(\theta)}{\Delta\theta} \tag{6}$$

From (6), an analytical solution for the torque can be obtained. W' is the co-energy, which can be expressed as:

$$W' = \int_0^i \lambda \, di \tag{7}$$

And the motion equation is:

$$T_e = J\frac{\partial W}{\partial t} + D\omega + T_L \tag{8}$$

$$\omega = \frac{d\theta}{dt} \tag{9}$$

Where T_L, T_e, J, ω and D are load the electromagnetic torque, the rotor speed, the rotor inertia and the friction coefficient respectively.

The equations which have been mentioned above, can be combined together to build the simulation model for a SRM system. However, the function of inductance needs to be obtained by using a finite element method or by doing experiments with a prototype motor.

1.3 Torque control in Switch Reluctance Motor

The torque in SRM is generated toward the direction that the reluctance being to minimized. The magnitude of torque generated in each phase is proportional to the square of the phase current which controlled by the converter or drive circuit, and the torque control scheme. The drive circuit and torque control scheme directly affected to the performance and characteristic of the SRM. Many different topologies have emerged with a reduced number of power switch, faster excitation, faster demagnetization, high efficiency, high power factor and high power through continued research. Conventionally, there has always been a trade-off between gaining some of the advantages and losing some with each new topology.

The torque is proportional to the square of current and the slope of inductance. Since the torque is proportional to the square of current, it can be generated regardless of the direction of the current. And also because the polarity of torque is changed due to the slope of inductance, a negative torque zone is formed according to the rotor position. To have a motoring torque, switching excitation must be synchronized with the rotor position angle. As shown in Fig. 8, an inductance profile is classified into three regions, increasing ($\theta_{min1} \sim \theta_{max1}$), constant ($\theta_{max1} \sim \theta_{max2}$) and decreasing ($\theta_{max2} \sim \theta_{min2}$) period. If a constant exciting current flows through the phase winding, a positive torque is generated. When that is operated in inductance increasing period ($\theta_{min1} \sim \theta_{max2}$) and vice-versa in inductance decreasing ($\theta_{max2} \sim \theta_{min2}$).

In the case of a constant excitation, it cannot be generated any torque, because a positive torque and negative one are canceled out, and the shaft torque becomes zero. As a result, to achieve an effective rotating power, switching excitation must be synchronized with the inductance profile. In order to derive the phase current from (3), exact information about the inductance profile of the SRM is essential. In (10), the first term of the right side is voltage drops of winding resistance, the second term is the voltage drop of reactance and the last term is both the emf (electromotive magnetic force) and the mechanical output.

$$V = Ri + i(t)\frac{d\mathcal{L}(\theta,i)}{d\theta}\omega + \mathcal{L}(\theta,i)\frac{di(t)}{dt} \tag{10}$$

(a) Inductance profile

(b) Torque zone
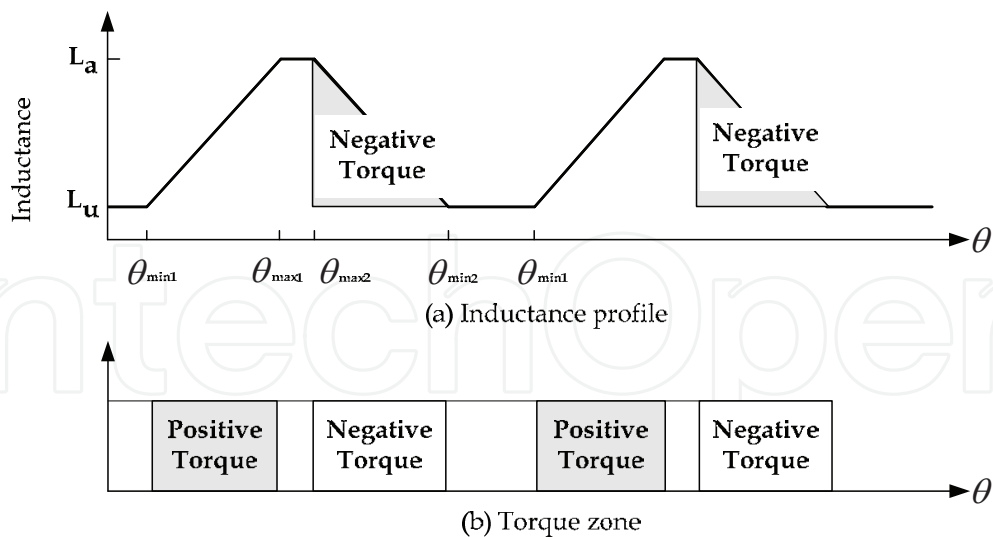
Fig. 8. (a)Inductance profile and (b) Torque zone

where, ω is the angular speed of the rotor.

In (10), the second in the right side can be considered as the back-emf; therefore, this term is expressed as:

$$e = \frac{d\mathcal{L}(\theta,i)}{d\theta}\omega i(t) = K\omega i(t) \tag{11}$$

$$\text{where, } K = \frac{d\mathcal{L}(\theta,i)}{d\theta} \tag{12}$$

As shown in (11), the back-emf equals to that of the DC motor. And also torque equation in (12) is equivalent with that of the DC series motor; therefore, the speed-torque of the magnetic energy in SRM is different from that of a mutual torque machine. And it operates more saturated level. The field energy in the magnetization curve is shown in Fig. 9.
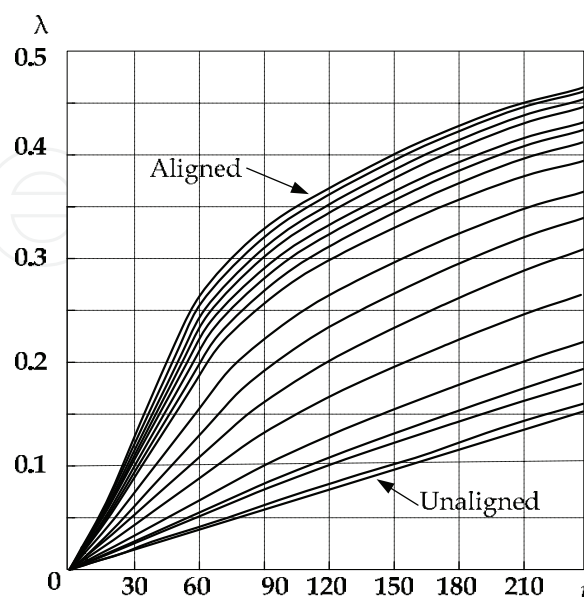

Fig. 9. Magnetizing curve and flux-linkage curve of SRM

It shows the magnetization curves from an aligned to an unaligned position. In SRM design, when poles of a rotor and a stator are aligned, the other phases are unaligned. In an aligned position, it has a maximum inductance with magnetically saturated easily. On the other hand, in an unaligned position it has a minimum inductance. As magnetic saturation is proportional to a rotor position, the magnetization curve according to the rotor position is an important factor to investigate the motor characteristics and to calculate the output power. The torque produced by a motor can be obtained by considering the energy variation. The generated torque is as:

$$T = [\frac{dW'}{d\theta}]_{i=const.} \tag{13}$$

where, w' means the co-energy, and it is given as:

$$W' = \int_0^i \lambda \, di \tag{14}$$

Under a constant phase current as shown in Fig. 10, when the rotor and total flux linkage are shifted from A to B, the SRM exchanges energy with the power source; thus, the stored field energy is also changed. The limitation to a constant current is that mechanical work done during the shifting region is exactly equal to the variation of co-energy. At a constant current, if the displacement between A and B is AB, the variation of energy received from the source can be expressed as:

$$\Delta W_e = ABCD \tag{15}$$

$$\Delta W_c = OBC - OAD \tag{16}$$

Then the mechanical work can be written as:

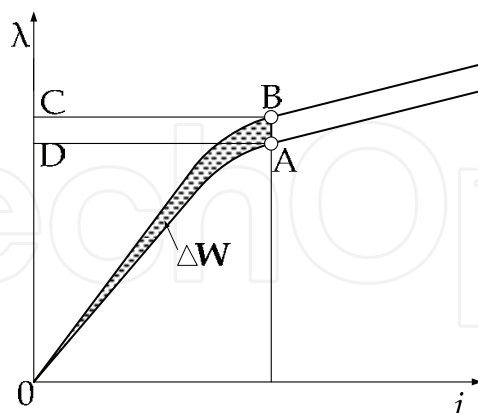$$\Delta W_m = T\Delta\theta = \Delta W_e - \Delta W_c = OAB \tag{17}$$

Fig. 10. Calculation of instant torque by the variation of co-energy at constant current

The above equation just shows the instantaneous mechanical output; therefore, in order to understand the characteristics of the motor, the average torque generated during an energy conversion cycle may be considered. The mechanical output is expressed as an area in an energy conversion curve (i-λ graph), the processes are separated with two stages as shown in Fig. 11.
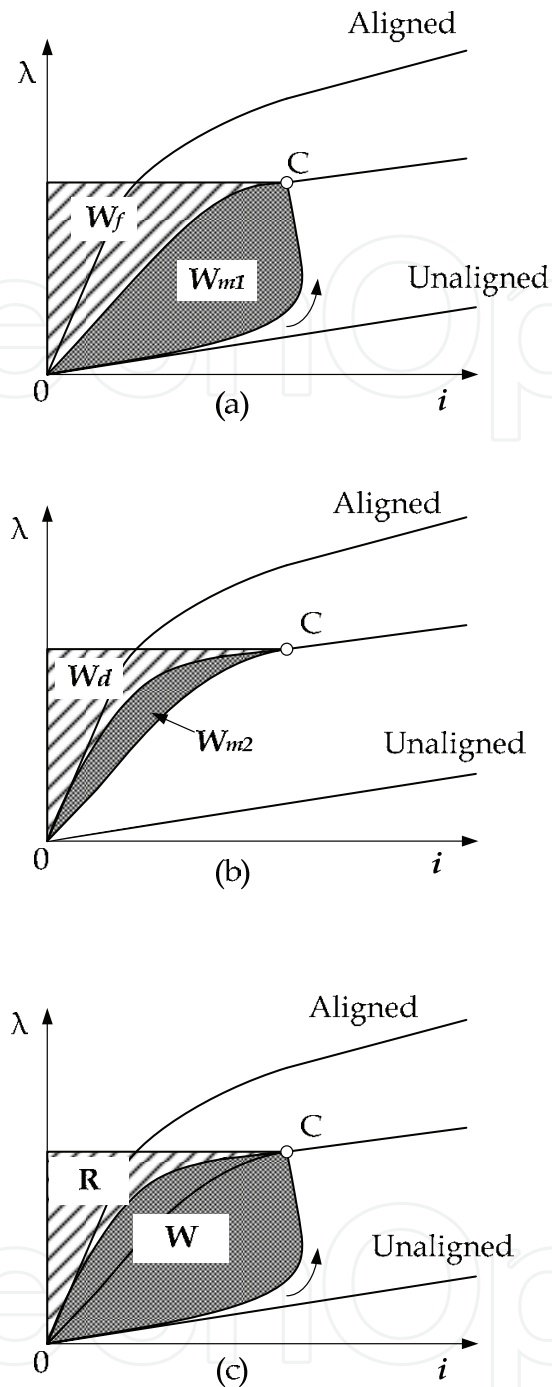
Fig. 11. Average torque (Energy conversion loop)

The total flux linkage is increased with phase current and inductance. Its operating area (i, λ) follows the curve between 0 and C as shown in Fig. 11(a). When the total flux linkage exists at point C, the mechanical work and stored energy between 0 and C becomes W_{m1} and W_f, respectively. Therefore, the total energy received from the source is summed up the mechanical work and the stored energy. On the other hand, when the demagnetizing voltage is applied at the point C, terminal voltage becomes negative; then current flows to the source through the diode. Its area follows the curve between C and 0 in Fig. 11(b). During process, some of the stored energy in SRM are appeared as a mechanical power;.

During the energy conversion, the ratio of supply and recovered energy considerably affects to the efficiency of energy conversion. To augment the conversion efficiency, the motor must be controlled toward to increase the ratio. Lawrenson [Lawrenson,1980]] proposed the energy ratio E that explains the usage ability of the intrinsic energy.

$$W = W_{m1} + W_{m2} \tag{18}$$

$$R = W_d = W_f - W_{m2} \tag{19}$$

The energy ratio is similar to the power factor in AC machines. However, because this is more general concept, it is not sufficient to investigate the energy flowing in AC machines. The larger energy conversion ratio resulted in decreasing a reactive power, which improves efficiency of the motor. In a general SRM control method, the energy conversion ratio is approximately 0.6 - 0.7.

$$E = \frac{W}{W+R} \tag{20}$$

In conventional switching angle control for an SRM, the switching frequency is determined by the number of stator and rotor poles.

$$f_e = \frac{1}{2} p_s p_r [Hz] \tag{21}$$

The general switching angle control has three modes, i.e., flat-topped current build-up, excitation or magnetizing, and demagnetizing. Each equivalent circuit is illustrated in Fig. 12.
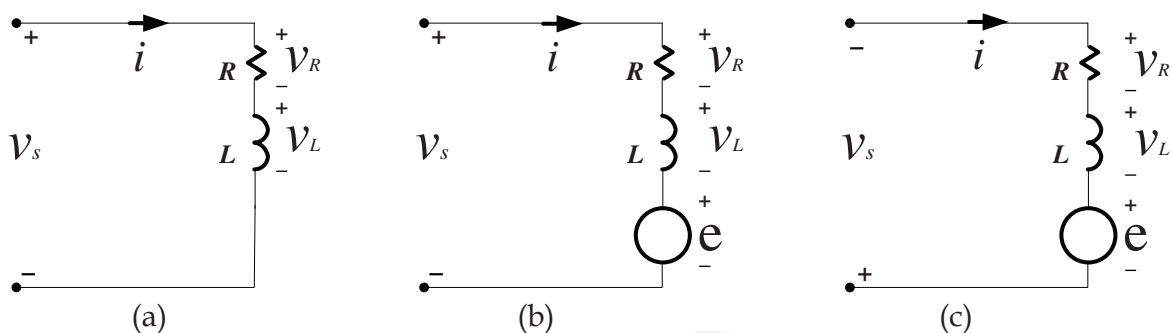

Fig. 12. Equivalent circuits when general switching angle control
(a) build-up mode (b) excitation mode (c) demagnetizing mode

Fig. 12(a) is a build-up mode for flat-topped current before inductance increasing. This mode starts at minimum inductance region. During this mode, there is no inductance variation; therefore, it can be considered as a simple RL circuit that has no back-emf. Fig. 12(b) shows an equivalent circuit at a magnetizing mode. In this mode, torque is generated from the built-up current. Most of mechanical torque is generated during this mode. A demagnetizing mode is shown in Fig. 12(c). During this mode, a negative voltage is applied to demagnetize the magnetic circuit not to generate a negative torque.

An additional freewheeling mode shown in Fig.13 is added to achieve a near unity energy conversion ratio. This is very effective under a light-load. By employing this mode, the energy stored is not returned to the source but converted to a mechanical power that is multiplication of phase current and back-emf. This means that the phase current is decreased by the back-emf.
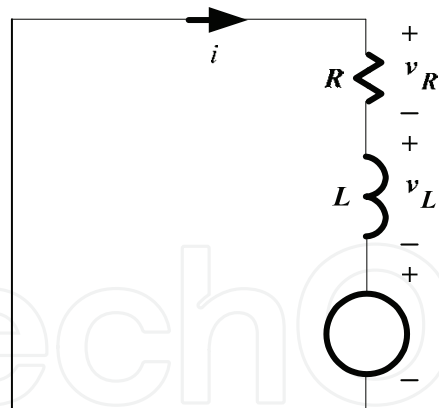
Fig. 13. Equivalent circuit of additional wheeling mode supplemented to conventional

If the increasing period of inductance is sufficiently large compared with the additional mode, the stored field energy in inductance can be entirely converted into a mechanical energy; then the energy conversion ratio becomes near unity.

1.4 Power converter for Switched Reluctance Motor

The selection of converter topology for a certain application is an important issue. Basically, the SRM converter has some requirements, such as:

* Each phase of the SR motor should be able to conduct independently of the other phases. It means that one phase has at least one switch for motor operation.
* The converter should be able to demagnetize the phase before it steps into the regenerating region. If the machine is operating as a motor, it should be able to excite the phase before it enters the generating region.

In order to improve the performance, such as higher efficiency, faster excitation time, fast demagnetization, high power, fault tolerance etc., the converter must satisfy some additional requirements. Some of these requirements are listed below.

Additional Requirements:

* The converter should be able to allow phase overlap control.
* The converter should be able to utilize the demagnetization energy from the outgoing phase in a useful way by either feeding it back to the source (DC-link capacitor) or using it in the incoming phase.
* In order to make the commutation period small the converter should generate a sufficiently high negative voltage for the outgoing phase to reduce demagnetization time.
* The converter should be able freewheel during the chopping period to reduce the switching frequency. So the switching loss and hysteresis loss may be reduced.
* The converter should be able to support high positive excitation voltage for building up a higher phase current, which may improve the output power of motor.
* The converter should have resonant circuit to apply zero-voltage or zero-current switching for reducing switching loss.

1.4.1 Basic Components of SR Converter

The block diagram of a conventional SRM converter is shown in Fig. 14. It can be divided into: utility, AC/DC converter, capacitor network, DC/DC power converter and SR motor.
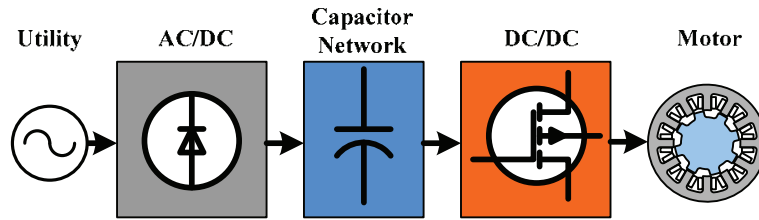
Fig. 14. Component block diagram of conventional SR drive

The converter for SRM drive is regarded as three parts: the utility interface, the front-end circuit and the power converter as shown in Fig. 15. The front-end and the power converter are called as SR converter.
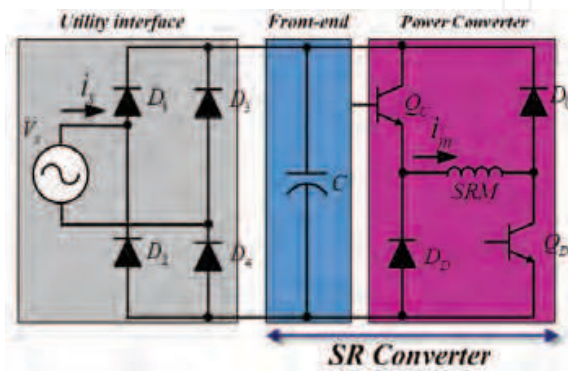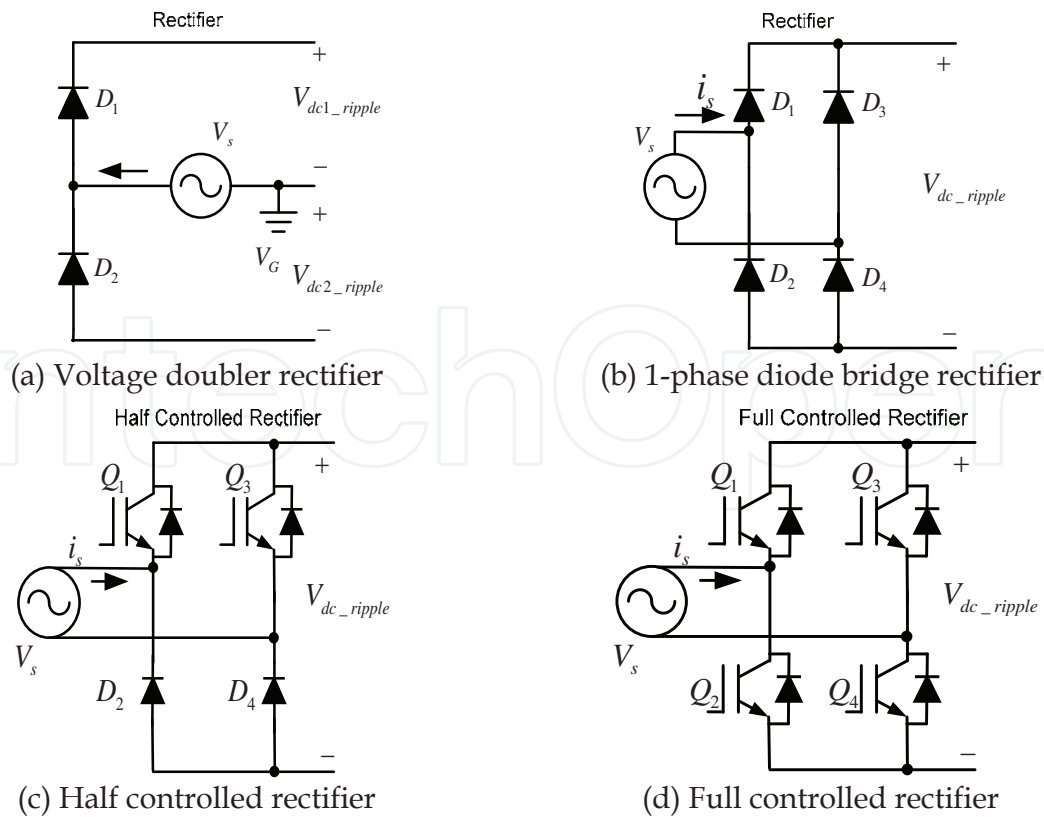

Fig. 15. Modules of SR Drive

(a) Voltage doubler rectifier

(b) 1-phase diode bridge rectifier

(c) Half controlled rectifier

(d) Full controlled rectifier

Fig. 16. Utility interface

A. Utility Interface

The main function of utility interface is to rectify AC to DC voltage. The line current input from the source needs to be sinusoidal and in phase with the AC source voltage. The AC/DC rectifier provides the DC bus for DC/DC converter. The basic, the voltage doubler and the diode bridge rectifier are popular for use in SR drives.

B. Front-end circuit

Due to the high voltage ripple of rectifier output, a large capacitor is connected as a filter on the DC-link side in the voltage source power converter. This capacitor gets charged to a value close to the peak of the AC input voltage. As a result, the voltage ripple is reduced to an acceptable valve, if the smoothing capacitor is big enough. However, during heavy load conditions, a higher voltage ripple appears with two times the line frequency. For the SR drive, another important function is that the capacitor should store the circulating energy when the phase winding returned to.
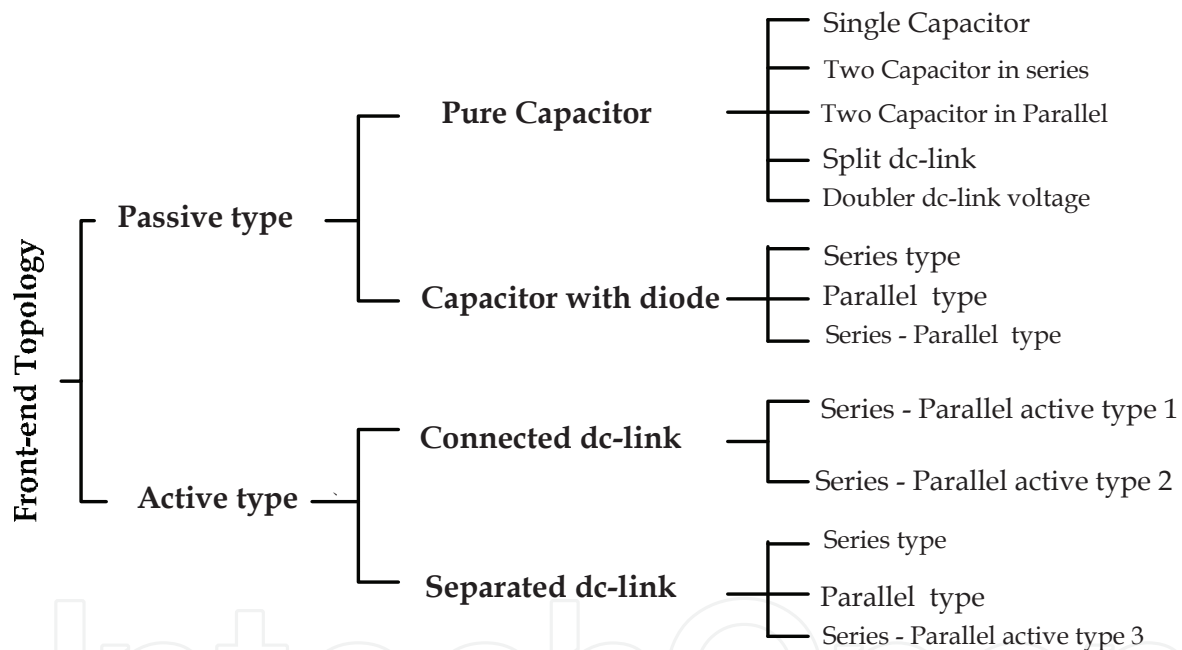

Fig. 17. Classification of capacitive type front-end topology

To improve performance of the SR drive, one or more power components are added. In this discussion, two capacitors networks are considered and no inductance in the front-end for reasonable implementation. Two types of capacitor network are introduced below: a two capacitors network with diodes and two capacitors with an active switch. The maximum boost voltage reaches two times the DC-link voltage.

The two capacitors network with diodes, which is a passive type circuit, is shown in Fig. 19. The output voltages of the series and parallel type front-ends are not controlled. Detailed characteristics are analyzed in Table 1.
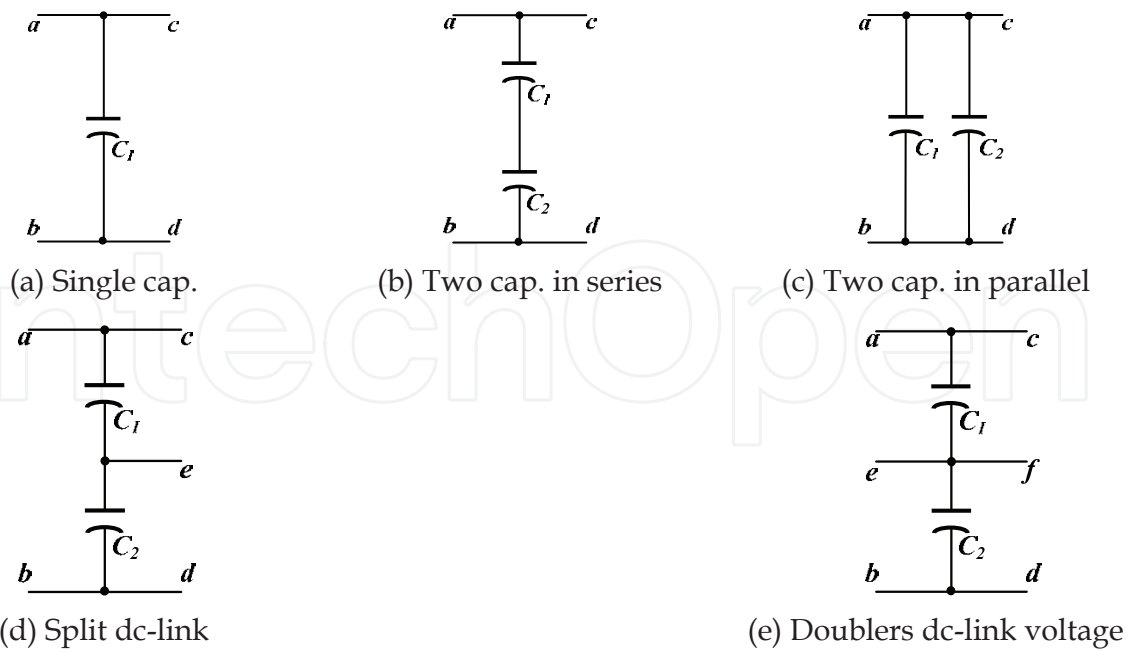
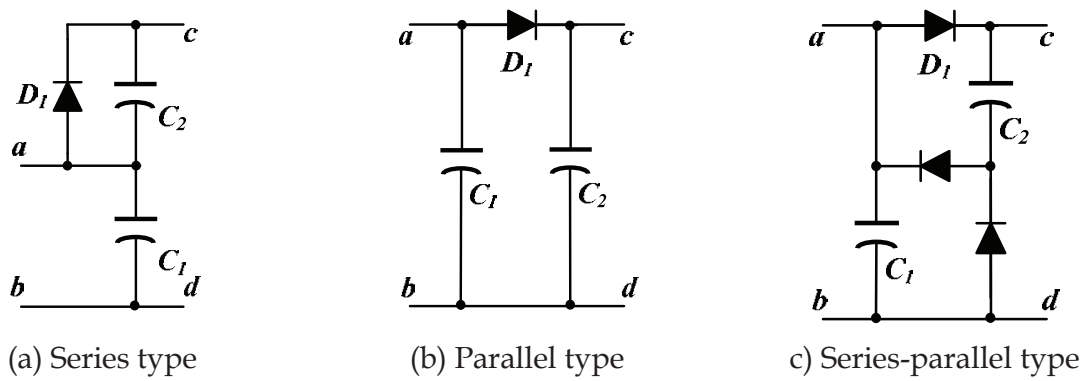(a) Single cap.   (b) Two cap. in series   (c) Two cap. in parallel

(d) Split dc-link   (e) Doublers dc-link voltage

Fig. 18. Pure capacitor network

(a) Series type   (b) Parallel type   c) Series-parallel type

Fig. 19. Two capacitors network with diodes

Type	Series	Parallel	Series-parallel
No. of Capacitor	2	2	2
No. of Diode	1	1	3
V_{boost}	$V_{C1}+V_{C2}$	V_{C2}	$V_{C1}+V_{C2}$
V_{dc}	V_{DC}	V_{DC}	V_{DC}
Spec. Boost Capacitor	V_{DC}	V_{boost}	V_{DC}
Spec. Diode	V_{DC}	V_{DC}	V_{DC}

Table 1. Characteristics of two capacitor network with diodes

The active type of the two capacitors network connected to the DC-link, which is a two output terminal active boost circuit, is shown in Fig. 20 and Table 2.
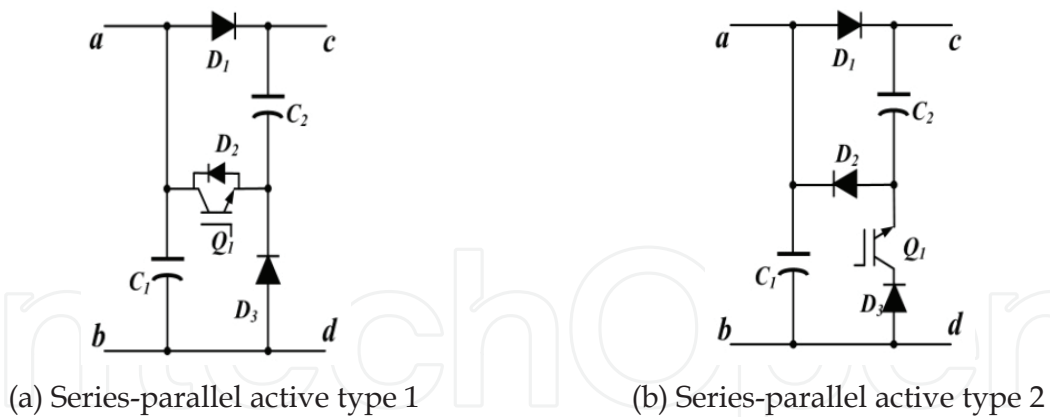
(a) Series-parallel active type 1   (b) Series-parallel active type 2

Fig. 20. Active type of two capacitors network connected to DC-link

Type	Series-parallel 1	Series-parallel 2
No. of Capacitor	2	2
No. of Switch	1	1
No. of Diode	2	3
V_{boost}	$V_{C1}+V_{C2}$	V_{C2}
V_{demag}	$-(V_{C1}+V_{C2})$	$-(V_{C1}+V_{C2})$
$Dc\text{-}link$	V_{DC}	V_{DC}
Spec. Boost Capacitor	V_{DC}	V_{boost}
Spec. Diode	V_{DC}	V_{DC}

Table 2. Characteristics of active type of two capacitors connected to DC-link

The active type of two capacitors network separated to DC-link is shown in Fig. 21 and Table 3.
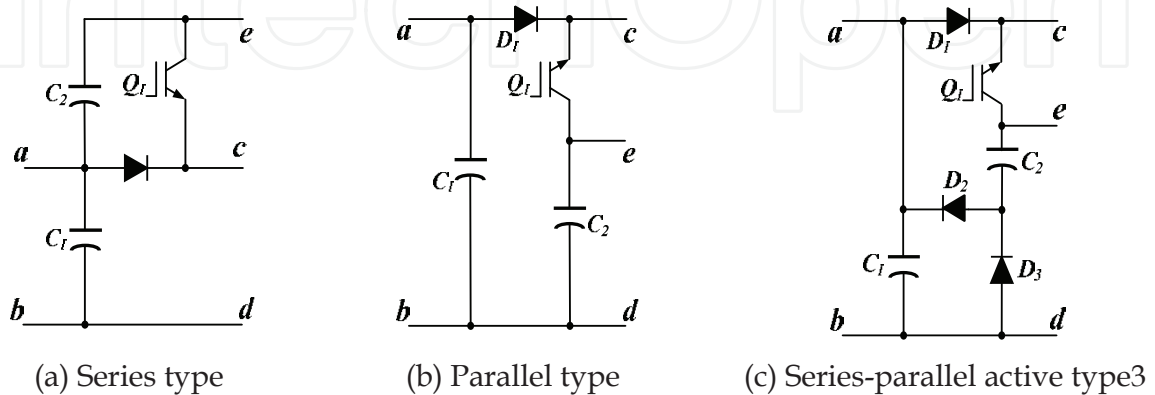

(a) Series type   (b) Parallel type   (c) Series-parallel active type3

Fig. 21. Active type of two capacitors network separated to DC-link

Type	Series	Parallel	Series-parallel type 3
No. of Capacitor	2	2	2
No. of Switch	1	1	1
No. of Diode	1	1	3
V_{boost}	$V_{C1}+V_{C2}$	V_{C2}	V_{C2}
V_{demag}	$-(V_{C1}+V_{C2})$	$-V_{C2}$	$-(V_{C1}+V_{C2})$
V_{dc}	V_{DC}	V_{DC}	V_{DC}
Spec. Capacitor	V_{DC}	V_{boost}	V_{C2}
Spec. Diode	V_{DC}	V_{DC}	V_{C2}

Table 3. Characteristics of active type of two capacitors separated to DC-link

C. Power converter

The power circuit topology is shown in Fig. 22 and Table 4. In this figure, five types of DC-DC converter are shown.
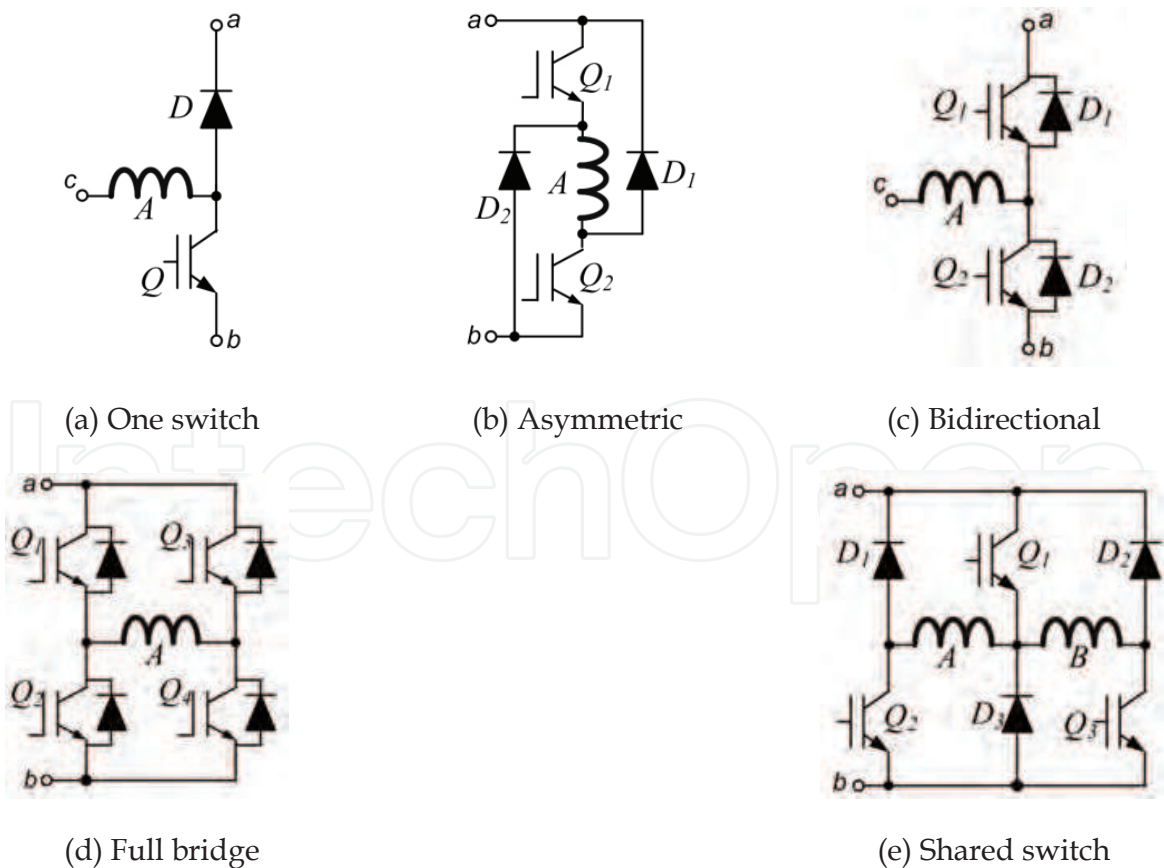

(a) One switch   (b) Asymmetric   (c) Bidirectional

(d) Full bridge   (e) Shared switch

Fig. 22. Active type of two capacitors network separated to DC-link

Type	One switch	Asymetric	Bi-directional	Full bridge	Shared switch
No. Switch	1	2	2	4	3
No. Diode.	1	2	0	0	3
No. Phase	1	1	1	1	2
$V_{Excitation}$	V_{dc}	V_{dc}	$V_{dc}/2$	V_{dc}	V_{dc}
$V_{Demagnetitation}$	V_{dc}	V_{dc}	$V_{dc}/2$	V_{dc}	V_{dc}
Current Direction	Uni.	Uni.	Bi.	Uni.	Uni.

Table 4. Comparison of 5 types of DC/DC converter topology

1.4.2 Classification of SR converter

One of the well-known classifications of SRM converters only considering the number of power switches and diodes is introduced [miller,1990]. Different from the classification, a novel classification, which focuses on the characteristics of converters, is proposed in [Krishnan,2001].

A. SR converter by phase switch

The classification of power converter focuses on the number of power switches and diodes. These options have given way to power converter topologies with q, (q+1), 1.5q, and 2q switch topologies, where q is the number of motor phases. These configurations are classified and listed in Fig. 23 for easy reference. A two-stage power converter configuration which does not fit this categorization based on the number of machine phases is also included.
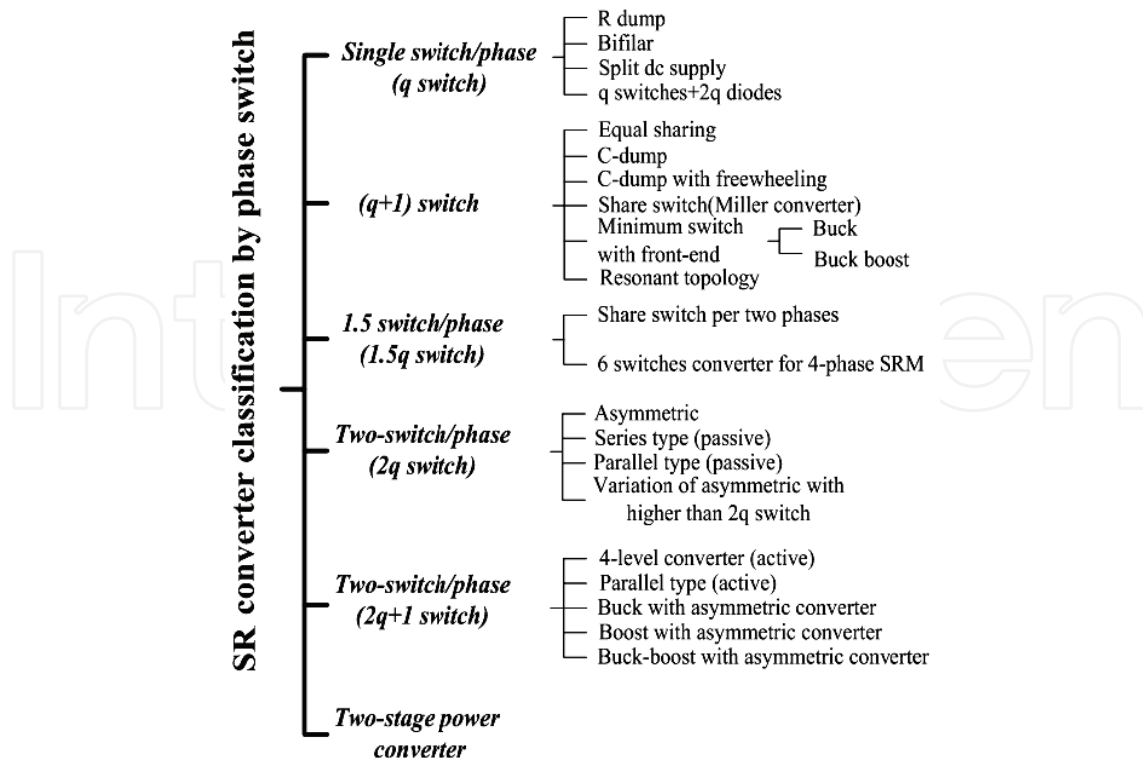

Fig. 23. SR converter classification by phase switch

All the converter topologies, except the two-stage power converter, assume that a DC voltage source is available for their inputs. This DC source may be from batteries or most usually a rectified AC supply with a filter to provide a stable DC input voltage to the SR converters.

Even though it is easy with the classification to find the number of semiconductors and the cost by counting the number of active components, it does not show important characteristics of a power converter, and the voltage ratings for the power switches and diodes are difficult to consider.

B. SR converter by commutation

Different converters which have the same number of switches may obtain different performance and characteristics. From this point of view, such a classification is not useful for finding the characteristic of an SRM converter.

The three types in the classification were presented as: extra commutation, half bridge and self commutation. In the extra commutation circuit, the capacitive, the magnetic and dissipative circuit is included. However, the distinction between three types in the classification is not clearly defined. Conventionally, the half bridge and the self commutation circuit also need a large capacitor in the front-end. They could also be classified as capacitive circuit. Moreover, the characteristic of circuits which contain one or more inductances is not shown in the classification.
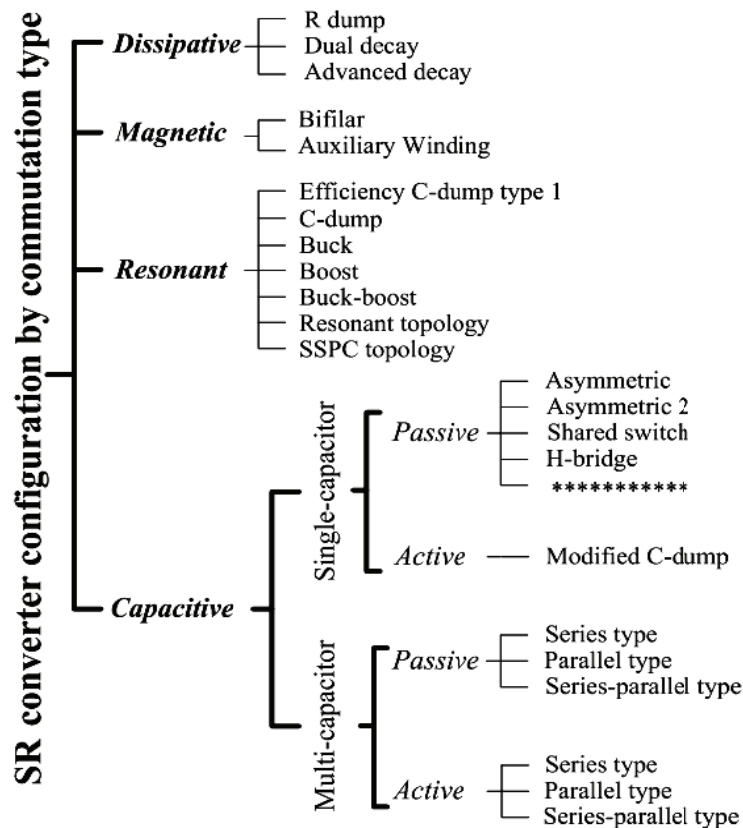

Fig. 24. SR converter configuration by commutation type

An SR converter configuration by commutation type is shows in Fig. 24. Based on the commutation type of the most of the returned or dissipated stored magnetic energy, the four major sorts are classified: dissipative, magnetic, resonant and capacitive type. Because the

capacitive type is focused in this discussion, the capacitive converter category is split into several subclasses. The concepts for passive and active converters are introduced. The distinction between active and passive is determined by whether they include a controllable power switch or not.

1. Dissipative converter

The dissipative type dissipates some or all of the stored magnetic energy using a phase resistor, an external resistor or both of them. The remaining energy is transformed to mechanical energy. Therefore, none of the stored magnetic energy in the phase winding is returned to DC-link capacitor or source. The advantage of this type of converter is that it is simple; a low cost and has a low count of semiconductor components.

(a) R-dump   (b) Zener-dump

Fig. 25. Two types of dissipative SR converter

2. Magnetic converter

The magnetic type is where the stored magnetic energy is transferred to a closely coupled second winding. Of course, that energy could be stored in DC-link capacitor or used to energize the incoming phase for multi-phase motors or use special auxiliary winding. The major advantage is a simple topology. The one switch per phase power circuit can be used. However, the potential rate of change of current is very high due to the stored magnetic energy is recovered by a magnetic manner. And the coupled magnetic phase winding which should be manufactured increases the weight of copper and cost of motor. Moreover, the power density of the motor is lower than that of the conventional ones.
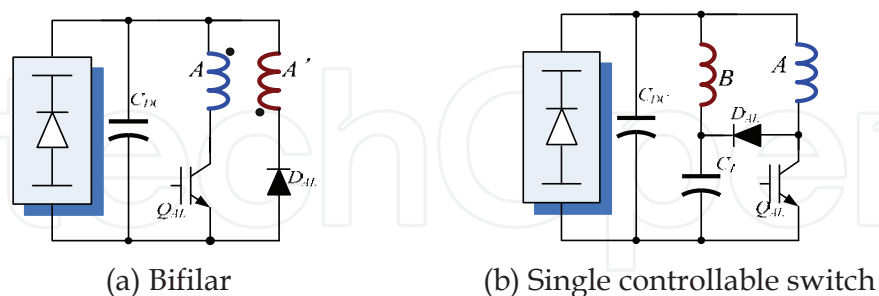

(a) Bifilar   (b) Single controllable switch

Fig. 26. Two types of magnetic SR converter

3. Resonant converter

The resonant type has one or more external inductances for buck, boost or resonant purposes. Conventionally, the inductance, the diode and the power switch are designed as a snubber circuit. So, the dump voltage can be easily controlled, and the low voltage is easy to boost. In a special case, an inductance is used to construct a resonant converter. The major advantage is that the voltage of phase winding can be regulated by a snubber circuit. However, adding an inductance increases the size and cost of converter. The other

additional components also increase the cost of converter. Three types of resonant type are shown in Fig. 27. All of them use a snubber circuit, which is composed by a power switch, a diode and an inductance.
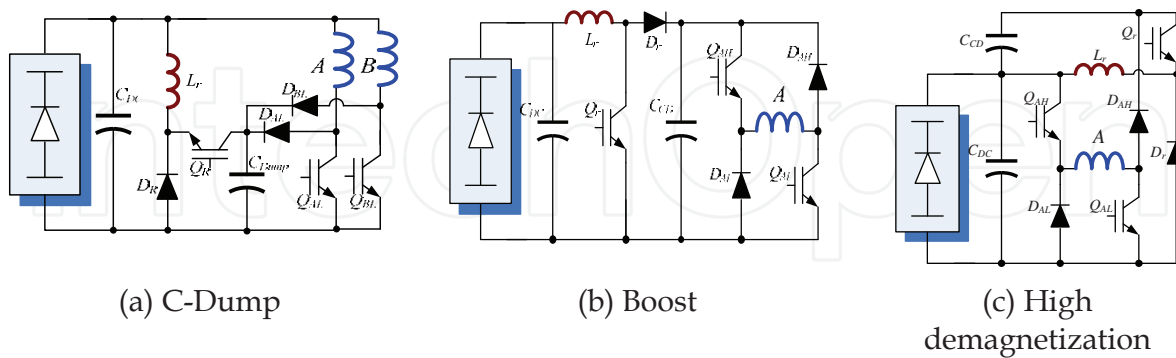

(a) C-Dump   (b) Boost   (c) High demagnetization

Fig. 27. Three types of resonant SR converter

4.   Capacitive converter

The magnetic energy in the capacitive converters is fed directly back to the boost capacitor, the DC-link capacitor or both of the capacitors. Compared to the dissipative, magnetic, and resonant converters, one component is added in the main circuit. So, this component will increase the loss of the converter. Different from the other converters, the stored magnetic energy can easily be fed back using only the inductance of phase winding. Although the capacitor has an equivalent series resistance (ESR), the loss of ESR is lower than that of other converters. Therefore, the capacitive converter is more effective for use in SR drive.
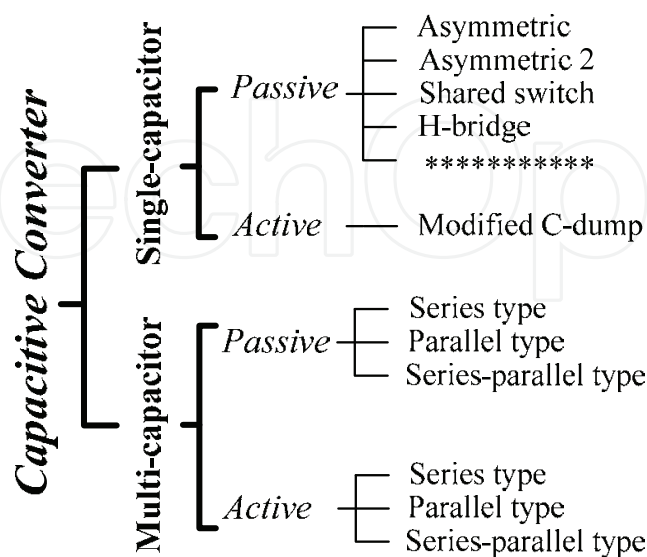

Fig. 28. Classification of capacitive SR converter

(a) Asymmetric

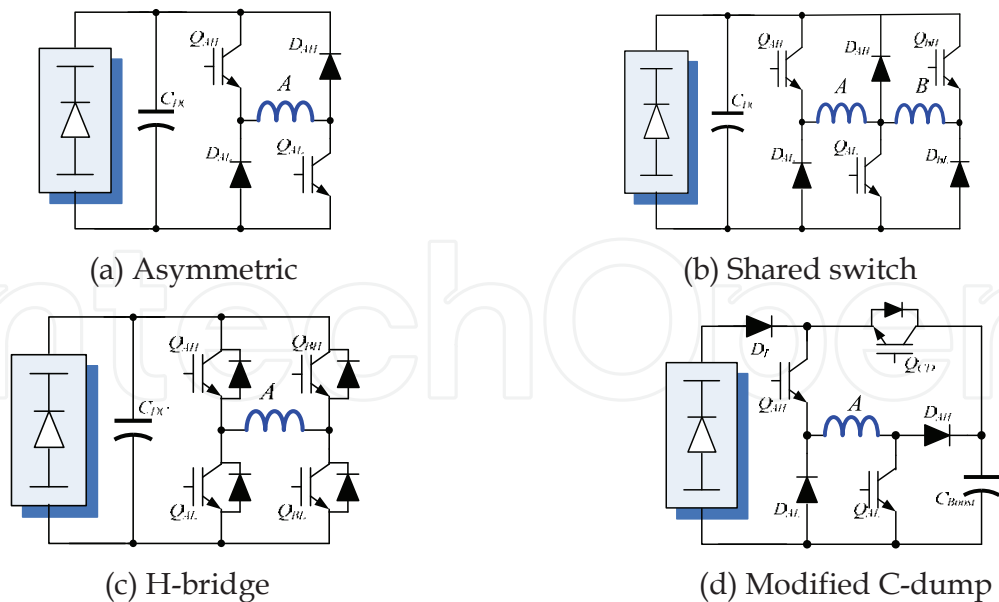(b) Shared switch

(c) H-bridge

(d) Modified C-dump

Fig. 29. Single capacitor type in capacitive SR converter

The capacitive converter can be divided two sorts: single capacitor and multi-capacitor type.

i.   Single-capacitor converter

Single-capacitor converters have simple structure, which makes them very popular. Four single capacitor types are shown in Fig. 29. One capacitive converter has as a simple front-end as shown in Fig. 29(a)-(c). This capacitor should be large enough to remove the voltage ripple of the rectifier and store the magnetic energy. Since the DC-link capacitor voltage is uncontrollable during charging and discharging, this type of converter is defined as a passive converter. The modified C-dump converter is shown in Fig. 29(d). In this converter, the boost capacitor only stores the recovered energy to build up a boost voltage. Unfortunately, one power switch should be placed in front of the boost capacitor to control the voltage. Because the boost capacitor does not reduce the DC-link voltage from the rectifier, the fluctuating DC-link voltage is input directly to the phase winding. The boost capacitor has only to be big enough for the stored magnetic energy, so the size of this capacitor is smaller than that of conventional DC-link capacitor. The Single capacitor in capacitive converters simplifies the construction of the converter. However, the input voltage for the phase winding is kept fixed by the DC-link capacitor. If only a boost capacitor is used, the DC-link voltage is fluctuating, and one power switch is added to control the boost voltage. This extra switch may increase the cost of converter.

ii. Multi-capacitor converter

Multi-capacitor converters include two or more capacitors in the converter topology to obtain boost voltage. Extra capacitors may make the topology of converter more complex. In this discussion, different converter topologies, which include two capacitors, are considered. The different types of passive type front-ends are shown in Fig. 30. The passive converter with two capacitors in parallel type is in Fig. 30(a). Due to the direction of diode, the stored magnetic energy is only feed back to the boost capacitor. The maximum boost voltage can be obtained by a suitable size of the capacitor. Because the discharge of the boost capacitor is not controllable in the passive converter, the voltage of the boost capacitor is changed by the stored magnetic energy

during different operating condition. When the phase switch is turned on, the voltage of the boost capacitor may fall very fast until the voltage reaches the DC-link voltage. Due to the non-linear characteristic of the SR motor, it is difficult to estimate advance angle or turn-on angle.

A passive converter with two capacitors in series is shown in Fig. 30(b). The stored magnetic energy charges the two capacitors in series. So, a part of the energy is stored in the boost capacitor to build up a boost voltage. It has the same advantage as for the parallel passive converter. However, the voltage rating of the boost capacitor is less than that of the parallel converter.

(a) Parallel type   (b) Series type

(c) Series-parallel type
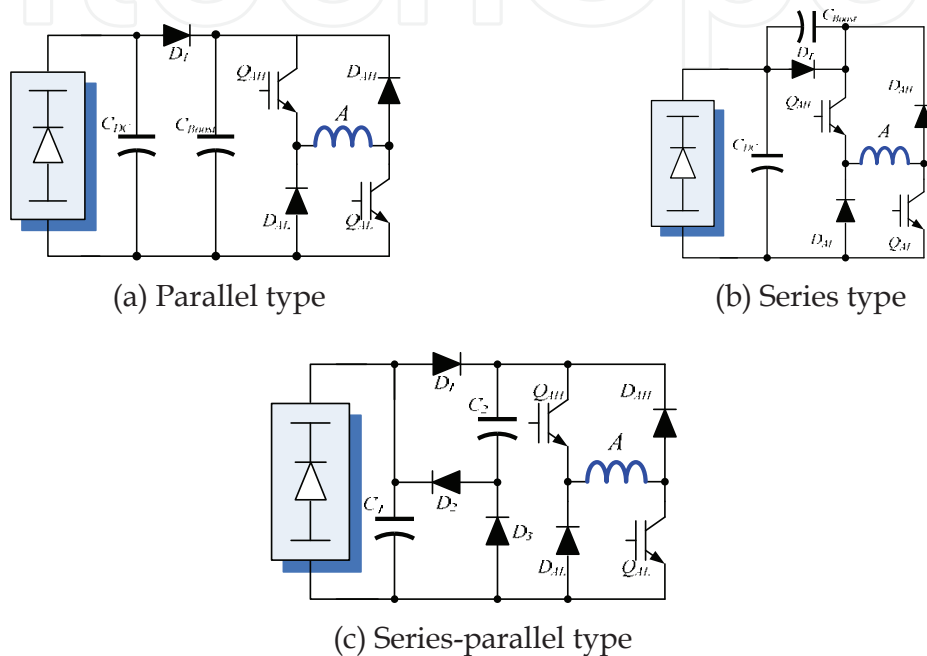
Fig. 30. Passive boost converter with two capacitors

Another passive converter of two capacitors in series-parallel type is in Fig. 30(c). This converter is made of rectifier, the passive boost circuit and an asymmetric converter. The excitation voltage is the DC-link voltage, but the demagnetization voltage is twice of DC-link voltage. The high demagnetization voltage can reduce the tail current and negative torque; it could also extend the dwell angle to increase the output.

(a) Split dc-link type   (b) Doublers dc-link voltage type
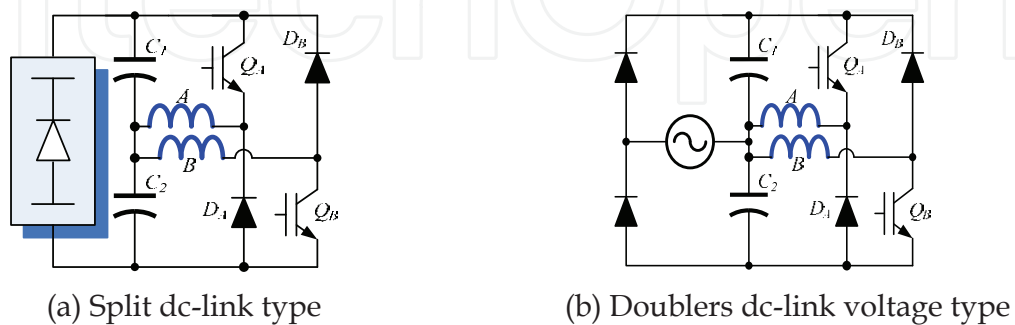
Fig. 31. other passive SR converter with series capacitor type

Other passive SR converter with two series capacitors is shown in Fig. 31. The front-end and DC-DC converter are same, but the bridge rectifier and the voltage doubling rectifier are

connected. The split DC-link converter is shown in Fig. 31(a). The phase voltage of this converter is a half of DC-link voltage. The double dc-link voltage converter is shown in Fig. 31(b). The phase voltage is same to DC-link voltage. The main advantage of these two converters is that one switch and one diode per phase is used. However, the voltage rating of power switch and diode is the twice the input excitation voltage.

The active boost converter with two capacitors connected in parallel is shown in Fig. 32. The four active boost converters with two capacitors connected in parallel are introduced. To handle the charging of the capacitor in the beginning of the conduction period, one diode is needed to series or parallel with the power switch to protect the power switch. When parallel type 1 and 2 are used with the asymmetric converter, the maximum voltage rating of the power diode and the switch is the same as the desired boost voltage. While the diode is connected to the power switch, the boost capacitor is only charged by the stored magnetic energy. In the beginning, the voltage of the boost capacitor is increased from 0 to the desired value. For the parallel converter of type 2, a diode in parallel with the power switch is used, so the boost capacitor can be charged by the DC-link capacitor. Parallel converters of type 3 and 4 which belong to capacitor dump converters are shown in Fig. 32(c) and (d). If the demagnetization voltage is required to be the same to DC-link, the voltage rating of power diode and switch is at least twice of DC-link voltage.

(a) Parallel type 1   (b) Parallel type 2

(c) Parallel type 3   (d) Parallel types 4
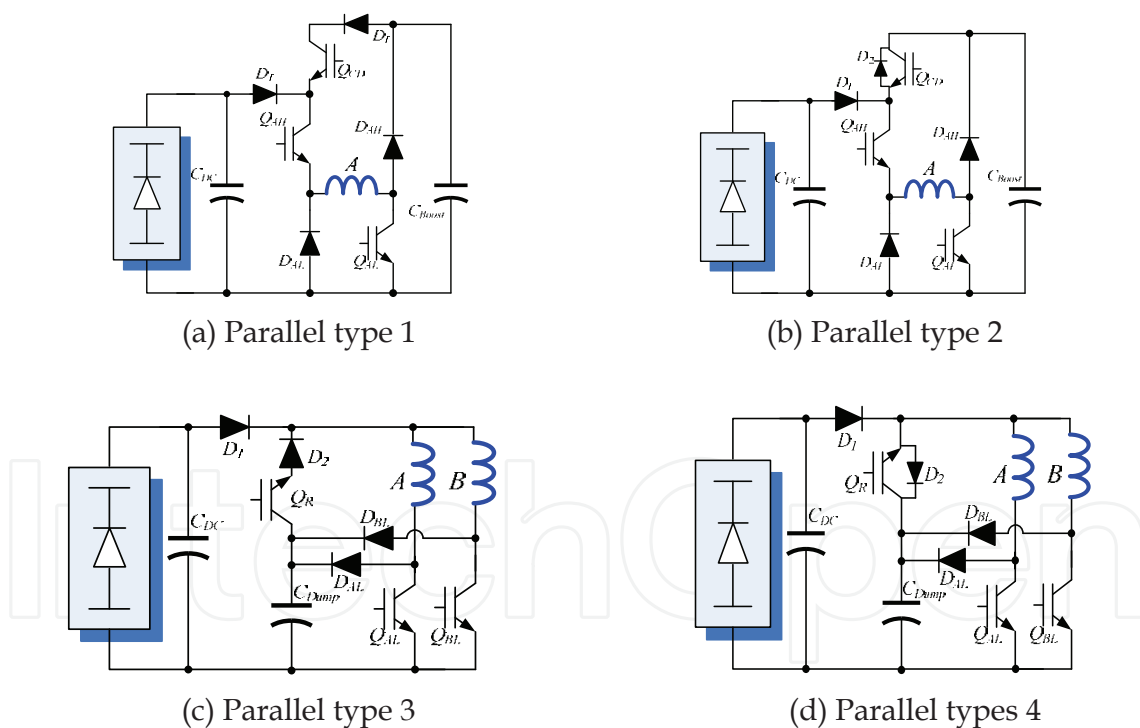
Fig. 32. Active boost converter with two capacitors connected in parallel

An active boost converter with two series connected capacitors is in Fig. 33(a). The stored magnetic energy charges the two series connected capacitors, so the boost voltage can be built up in the boost capacitor. The power switch Q_{cd} is used to control the boost voltage of the boost capacitor.

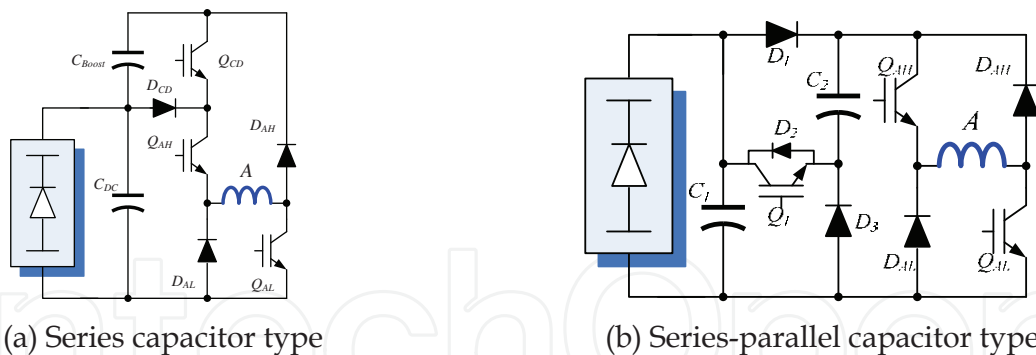(a) Series capacitor type   (b) Series-parallel capacitor type

Fig. 33. Active boost converter

An active boost converter with a series-parallel connection of the two capacitors is shown in Fig. 33(b). The active capacitor circuit added to the front-end consists of three diodes and one capacitor. This circuit combines a series-connected and a parallel-connected structure of two capacitors. Based on this active boost capacitor network, the two capacitors can be connected in series or parallel during different modes of operation. The operation mode of whole converter is presented in [Khrishnan,2001]. The fast excitation and demagnetization is easily obtained from the two series-connected capacitors. The stable voltage achieved with the two parallel-connected capacitors.

4 types of converter are compared in Table. 5. The converter with two capacitors connected in series or the converter with two capacitors connected in parallel may obtain a higher boost voltage than the series-parallel converter. However, an increased boost voltage may increase the cost of the converter. Since the series-parallel converter can limit the maximum voltage to twice the DC-link voltage, it is more stable and controllable.

	Asymmetric	2-capacitor in series type	2-capacitor in parallel type	2-capacitor in series-parallel
Vmax	Vdc	∞/2Vdc	∞/2Vdc	2Vdc
Vcontrol	No	Yes	Yes	optional
VC1_rate	Vdc	Vdc	Vdc	Vdc
VC2_rate	Vdc	∞/Vdc	∞/2Vdc	Vdc
No.Switch	2	3	3	3
No. Diode	2	3	3	4
Stability	Good	Normal	Normal	Good

Table 5. Comparison of 2-capacitor types

2. Torque control strategy

2.1 Angle control method

The switched reluctance drive is known to provide good adjustable speed characteristics with high efficiency. However, higher torque ripple and lack of the precise speed control are drawbacks of this machine. These problems lie in the fact that SR drive is not operated with an mmf current specified for dwell angle and input voltage. To have precise speed control with a high efficiency drive, SR drive has to control the dwell angle and input voltage instantaneously. The advance angle in the dwell angle control is adjusted to have high efficiency drive through efficiency test.

2.1.1 Switching angle control method

In SRM drive, it is important to synchronize the stator phase excitation with the rotor position; therefore, the information about rotor position is an essential for the proper switching operation. By synchronizing the appropriate rotor position with the exiting current in one phase; the optimal efficiency of SRM can be achieved. In this part various types of switching angle control method to achieve the optimal efficiency will be discussed.

A. Fixed angle switching method

Current source is a proper type to excite an SRM for its good feature of electromagnetic characteristics because it produces rectangular or flat-topped current and it is easy to control the torque production period. Therefore, it is considered as an ideal excitation method for switched reluctance machine but difficult and expensive to realize it.

To produce similar current shapes in voltage source, it is needed to regulate the supply voltage in the variable reluctance conditions. Usually PWM or chopper technique is used for this propose. But it is complex in its control circuit and increases loss. The other technique which is more simply in control is excitation voltage to form a flat-topped current by using fixed switching angle at various operation conditions. Fig. 34 shows excitation scheme with fixed switching angle control method.
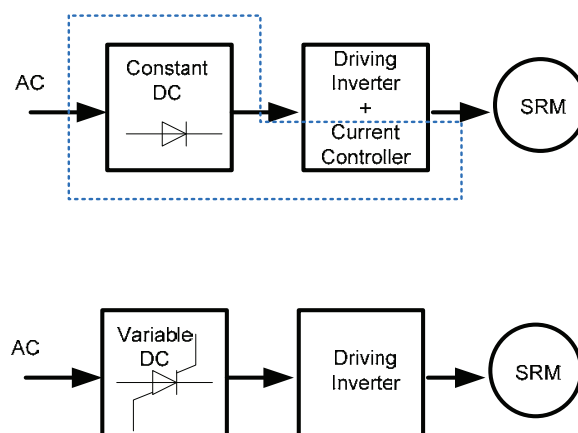
Fig. 34. Excitation scheme with fixed switching angle control method

In the fixed angle switching method, the turn-on angle and the turn-off angle of the main switches in the power converter are fixed; the triggering signals of the main switches are modulated by the PWM signal. The average voltage of phase winding could be adjusted by regulating the duty ratio of the PWM signal. So the output torque and the rotor speed of the motor are adjustable by regulating the phase winding average voltage.

Constant voltage source with current controller is substituted with variable voltage source to make the current flat-topped. Voltage equation of SRM for a phase is shown in (3). If winding resistance and magnetic saturation are ignored, an applied voltage to form a flat-topped current in the torque developed region is

$$V_c = K I_c \omega \tag{22}$$

Where V_c is amplitude of voltage, K is $dL/d\theta$, I_c is required current to balance load torque a, and ω is angular velocity. If magnetic saturation is considered, this equation is to be modified as

$$V' = \sigma K I_c \omega \tag{23}$$

Where σ is saturation factor. To calculate proper excitation voltage and switching angle for flat-topped current, let consider phase voltage and current as shown in Fig. 35. θ_{on} and θ_{off} are switching-on and switching-off angle, respectively. Phase current reaches to the desired value of current, I_c at θ_s, and become flat-topped current by this scheme, and the current decrease rapidly by reversing the applied voltage. θ_{off} is to be set in order to prevent the generation of negative torque. It can be divided into 3 regions to calculate the angles and voltages. In Region I and III, switching-on and switching-off angles are determined respectively. And in Region II, proper excitation voltage is calculated.
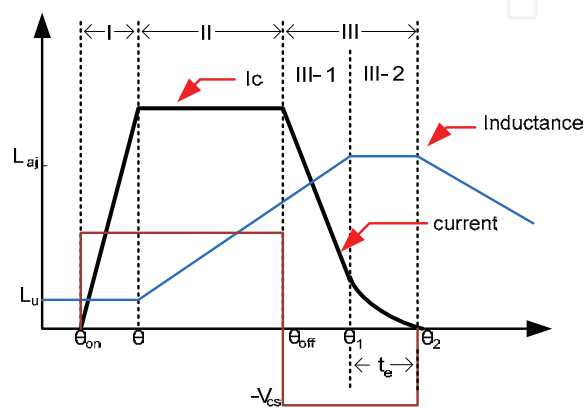
Fig. 35. Flat-topped phase current

• Region I : $\theta_{on} \leq \theta \leq \theta_s$ (switching-on angle determination)

θ_{on} is determined in this region. It is to ensure that current is to be settled to the desired value at θ_s. In this region, voltage equation becomes (24).

$$V_{cs} = Ri + L_u \frac{di}{dt} \tag{24}$$

Where L_u, is the minimum value of the inductance.

Required time, t_s to build up a phase current from 0 to I_c, which is the current to balance load torque, is derived from (23) and (24).

$$t_s = \frac{\theta_s - \theta_{on}}{\omega} = -\frac{L_u}{R} \ln(1 - \frac{R}{\sigma K \omega}) \tag{25}$$

Therefore, θ_{on} is

$$\theta_{on} = \theta_s - \frac{\omega L_u}{R} \ln(1 - \frac{R}{\sigma K \omega}) \tag{26}$$

θ_{on} is affected merely by saturation factor and not by speed variation except the range where speed is very low. Therefore, it can be fixed at the center of variation range of switching-on and compensate current build-up via applied voltage regulation for simple control.

• Region III : $\theta_{off} \leq 0 \leq \theta_t$ (Switching-off angle determination)

In this region, applied voltage must be reversed to accelerate current decay. It is divided into two sub-regions:

- Sub-region III-1

  Voltage and current equation are as follows.

$$-V_{cs} = Ri + L\frac{di}{dt} + \sigma K \omega i \tag{27}$$

$$i = I_c \left(2e^{-\frac{\sigma K\omega}{L}t} - 1\right) \tag{28}$$

These equations are effective only during $\theta_{off} \leq \theta \leq \theta_1$

- Sub-region III-2

  In this region, the inductance has its maximum value L_{aj} and is constant. So, current is

$$i = -\frac{V_{cs}}{L_{aj}} t + I_0 \tag{29}$$

Where I_0 is the current value at θ_1. This equation is effective during $\theta_1 \leq \theta \leq \theta_2$.

B. Advance angle control method

The SRM is controlled by input voltage, switch-on and switch-off angle. Switch-on and switch-off angle regulate the magnitude and shape of the current waveform. Also it results in affecting the magnitude and shape of the torque developed. To build up the current effectively with a voltage source, an advance switching before the poles meet is needed. The switch-on angle is one of the main factors to control the build-up currents. Therefore, this angle is controlled precisely to get optimal driving characteristics.
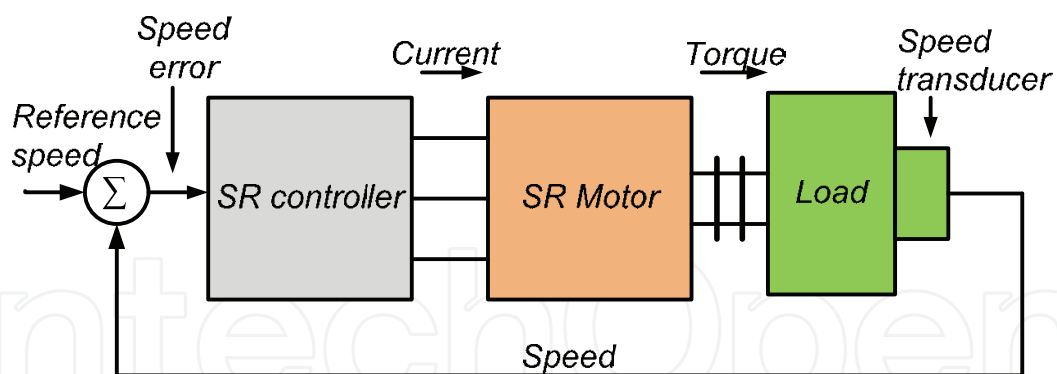
Fig. 36. Block diagram of advance angle control with feedback signal

In the real control system, control of advance angle which is controlled by variable load condition can be realized by simple feedback circuit using detecting load current. The block diagram of the advance angle control with a feedback signal shows in Fig.36.

The regulation of speed-torque characteristics of SRM drive is achieved by controlling advance angle and applied voltage. The advance angle is regulated to come up with the load variation in cooperation with the applied voltage.

The signal from the control loops is translated into individual current reference signal for each phase. The torque is controlled by regulating these currents. The feedback signal which is proportional to the phase detector is used to regulate the instantaneous applied voltage.

Variation relationship of torque with current or torque with rotor position must be compensated in the feed forward torque control algorithm. The relation between torques and current of a phase is shown in Fig. 37.
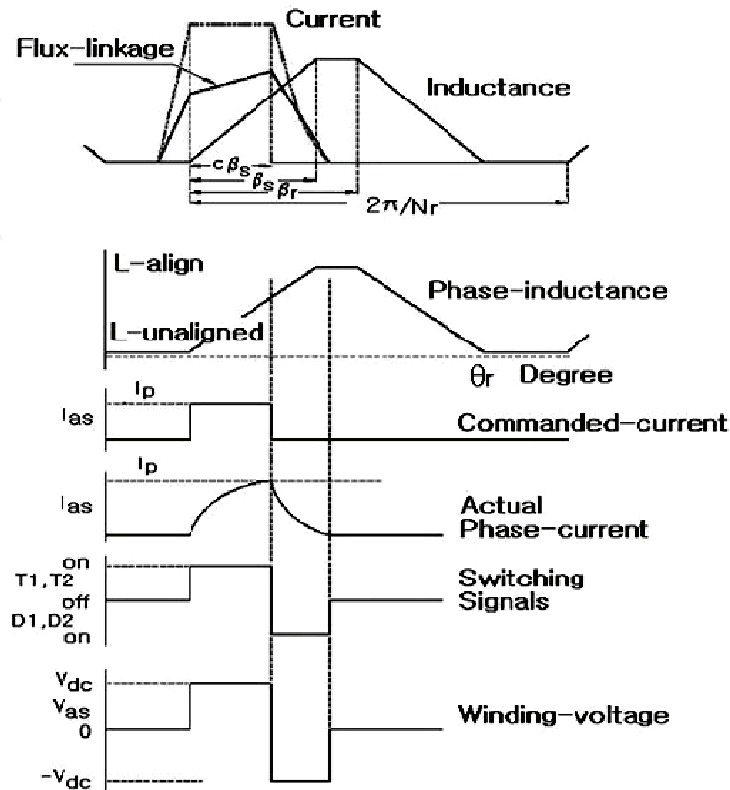

Fig. 37. Advance angle control

C. Switching-off angle control method

Control method of switch-off angle is introduced for variable load. The switching angle control method is based on two command signals for switching–on and switching–off angle independently. According to the motor speed and load condition, a proper switching-on angle θ_{on} is set at the cross point of negative slope of the sensor signal and the switching–on command signal V_{on} is

$$\theta_{on} = \left(1 - \frac{V_{on}}{V_{max}}\right)(\theta_0 - \theta_a) + \theta_a \tag{30}$$

The maximum switching-on angle is in the minimum inductance region. So, a fast build up of current is possible at the rated load. The minimum switching–on angle is in the increasing region of inductance. Therefore a smooth build up of current is possible at a light load with a smooth torque production. Similarly, the delay angle θ_{off} is set at the cross point of positive slope of the signal and the switching off command signal V_{off} as

$$\theta_{off} = \frac{V_{off}}{V_{max}}(\theta_d - \theta_0) + \theta_0 \tag{31}$$

In addition, the dwell angle is the interval of switching-on and switching–off angles, which takes the form

$$\theta_{dwell} = \theta_{off} - \theta_{on} \tag{32}$$

There are two types of control switch-off angle, one is constant torque angle (θ_{TQ}) control and the other is constant dwell angle (θ_{Dw}) control.

1.   Constant torque angle control

Torque angle is the angle between the increasing of inductance to the switching-off angle. This control method is fixed the turn-off angle and turn-on angle is tuned for a fluctuation of speed and load by constant torque angle control method. The fluctuation of efficiency is small until rated power, but if the turn-on angle moves toward for an increase torque, even in the region of decreasing inductance, the current will flow and negative torque will be produced. Thus, the efficiency becomes reduced. Therefore, it is needed to find a proper position of turn-on angle and the phase current which determined by constant torque angle control method.
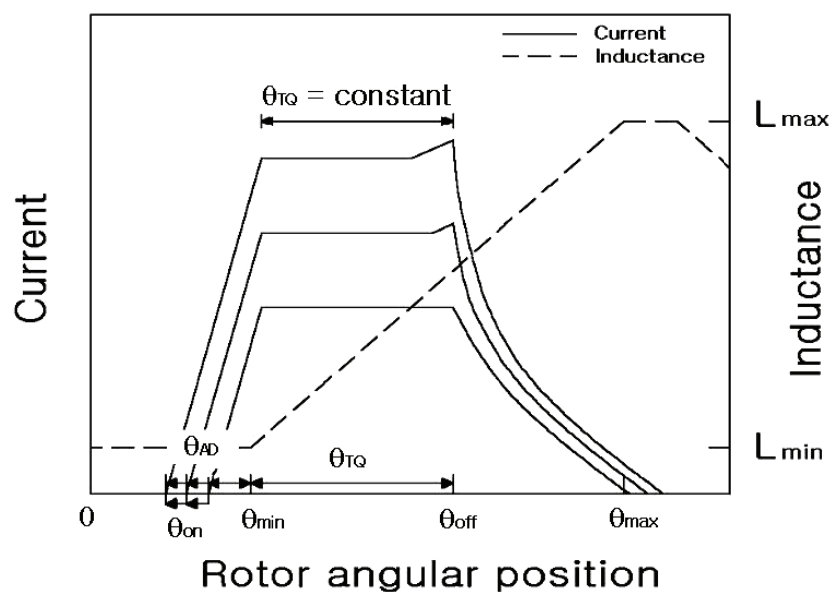
Fig. 38. Constant torque angle control

2.   Constant dwell angle control

The constant dwell angle method controls the turn-on or turn-off angle by keep constant dwell angle (θ_{Dw}) for speed or output control. When turn-on angle is moved to keep the constant speed, effect of negative torque is regardless of speed and load. But because of the limits of rated power, it can be unstable to drive on overload. This method makes a control system simple and easy to avoid negative torque in the switching-off region. Fig. 39 shows the relation between current and rotor position in constant dwell angle (θ_{Dw}) control.

2.1.2 Single pulse control method

Torque production in SRM is not constant and it must be established from zero at every stroke. Each phase must be energized at the turn-on angle and switched off at the turn-off angle. In the low speed range, the torque is limited only by the current, which is regulated

either by voltage-PWM or by instantaneous current. As the speed increases the back-EMF increases too, and there is insufficient voltage available to regulate the current; the torque can be controlled only by the timing of the current pulse. This control mode is called single-pulse mode.
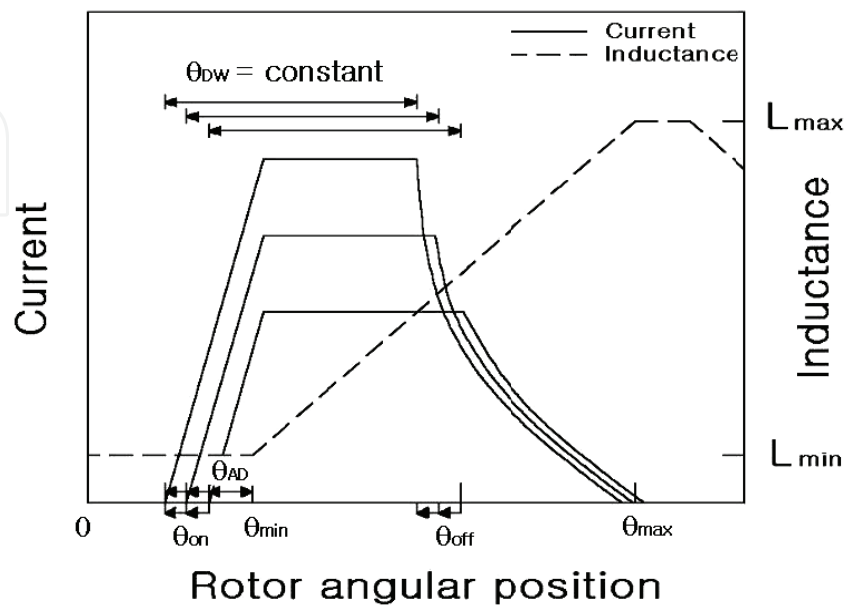

Fig. 39. Constant dwell angle (θ_{Dw}) control

In single pulse operation the power supply is kept switched on during the dwell angle and is switched off at the phase commutation angle. As there is no control of the current and a sharp increase of current, the amount of time available to get the desired current is short. Typically, single pulse operation is used at high mechanical speed with respect to the turn-on angle determined as a function of speed. Fig.40 shows the phase current in high speed region using an asymmetric converter. As shown in Fig. 40, SR drive is excited at θ_{on}
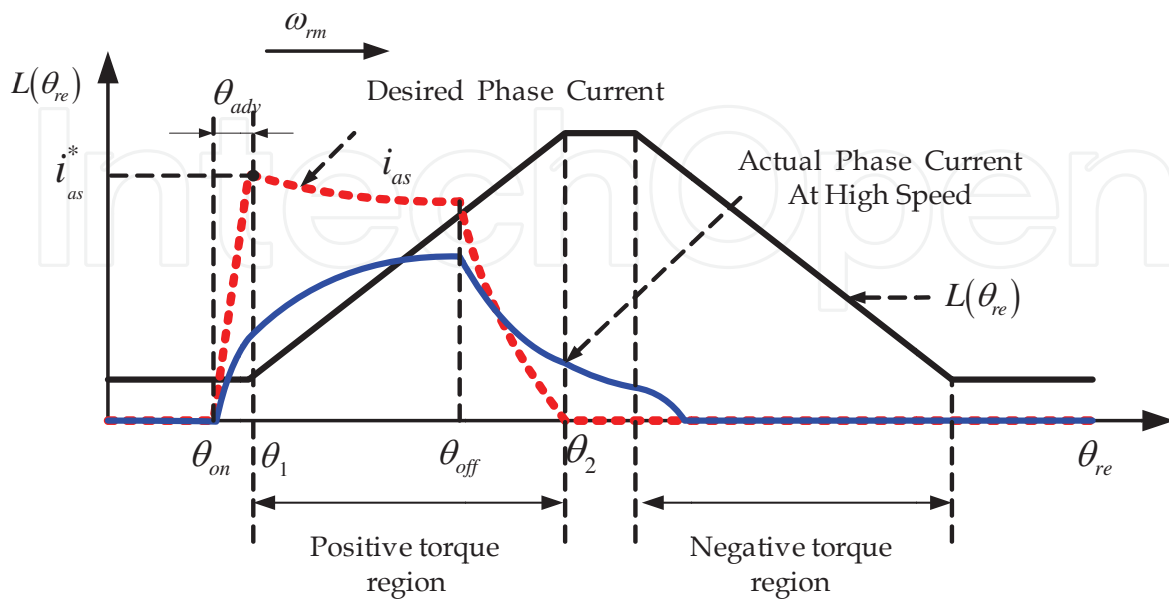
Fig. 40. Build-up of phase current in high speed region

position advanced as θ_{adv}, than the start point of positive torque region θ_1 in order to establish the sufficient torque current. The desired phase current shown as dash line in Fig. 40 is demagnetized at θ_{off}, and decreased as zero before the starting point of negative torque region θ_2 to avoid negative torque.

In order to secure enough time to build-up the desire phase current i^*_{as}, the advance angle θ_{adv} can be adjusted according to motor speed ω_m. From the voltage equations of SRM, the proper advance angle can be calculated by the current rising time as follows regardless of phase resistance at the turn-on position.

$$\Delta t = L(\theta_1).\frac{i^*_{abcs}}{V_{abcs}} \tag{33}$$

Where, i^*_{abcs} denotes the desired phase current of current controller and V_{abcs} is the terminal voltage of each phase windings. And the advance angle is determined by motor speed and (33) as follow

$$\theta_{adv} = \omega_m . \Delta t \tag{34}$$

As speed increase, the advance angle is to be larger and turn-on position may be advanced not to develop a negative torque. At the fixed turn-on position, the actual phase current denoted as solid line could not reach the desire value in high speed region as shown in Fig. 40. Consequently, the SRM cannot produce sufficient output torque. At the high speed region, turn-on and turn-off position are fixed and driving speed is changed. To overcome this problem, high excitation terminal voltage is required during turn-on region from θ_{on} to θ_1.

2.1.3 Dynamic angle control method

The dynamic angle control scheme is similar to power angle control in synchronous machine. When an SRM is driven in a steady-state condition, traces such as shown in Fig. 41(a) are produced. The switch-off instant is fixed at a preset rotor position. This may readily be done by a shaft mounted encoder. If the load is decreased, the motor is accelerated almost instantaneously. The pulse signal from a rotor encoder is advanced by this acceleration. This effect will reduce switch-off interval until the load torque and the developed torque balances [Ahn,1995]. Fig. 41(b) shows this action. On the contrary, if load is increased, the rotor will be decelerated and the switch-off instant will be delayed. The effect results in increasing the developed torque. Fig. 41(c) shows the regulating process of the dwell angle at this moment.

The principle of dynamic dwell angle is similar to PLL control. The function of the PLL in this control is to adjust the dwell angle for precise speed control. The phase detector in the PLL loop detects load variation and regulates the dwell angle by compares a reference signal (input) with a feedback signal (output) and locks its phase difference to be constant. Fig. 42 shows the block diagram of PLL in SR drive. It has a phase comparator, loop filter, and SRM drive.

The reference signal is a speed command and used for the switch-on signal. The output of the phase detector is used to control voltage through the loop filter. The switching inverter regulates switching angles. The output of phase detector is made by phase difference between reference signal and the signal of rotor encoder. It is affected by load variations. The dwell angle is similar to phase difference in a phase detector. To apply dynamic angle

control in an SR drive system, a reference frequency signals are used to switch-on, and the rotor encoder signal is used to switch-off similar to the function of a phase detector. The switch-off angle is fixed by the position of the rotor encoder. Therefore, the rotor encoder signal is delayed as load torque increased. This result is an increase of advance angle and initial phase current.
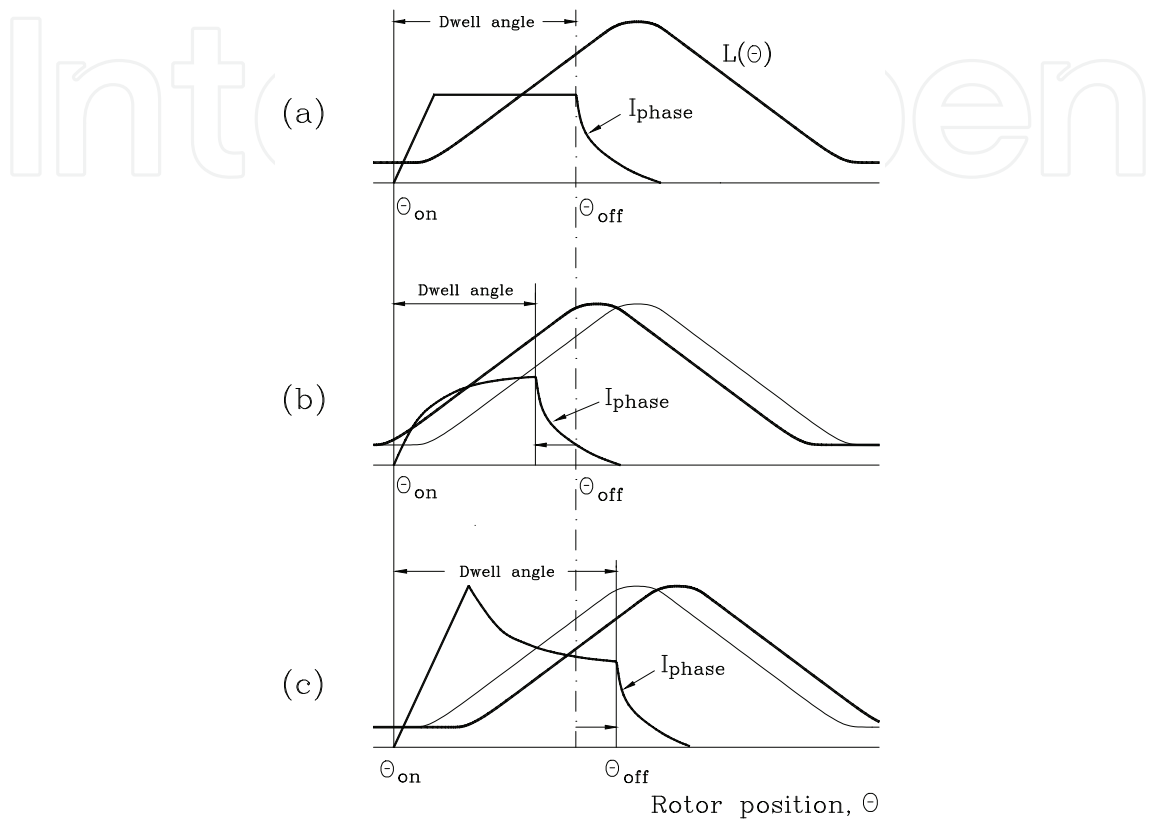

Fig. 41. Regulation of dwell angle according to load variation.
(a) steady-state. (b) load decreased. (c) load increased.
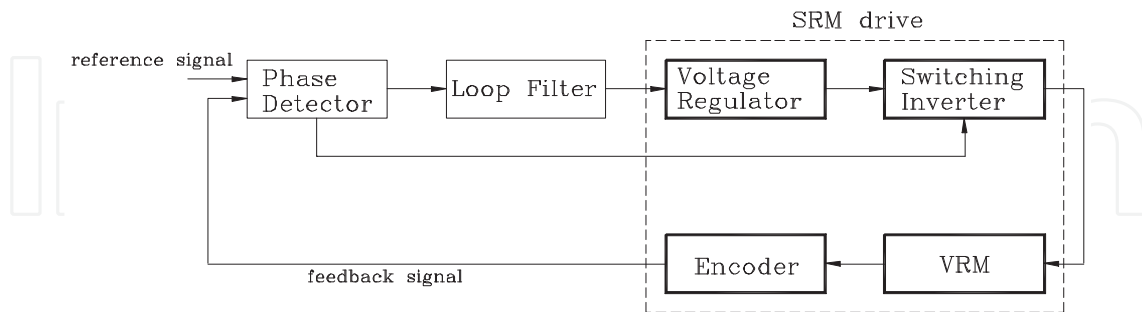
Fig. 42. Block diagram of PLL in SR drive.

2.2 Current control method

Control of the switched reluctance motor can be done in different ways. One of them is by using current control method. The current control method is normally used to control the torque efficiently. Voltage control has no limitation of the current as the current sensor is avoided, which makes it applicable in low-cost systems. Due to the development of

microcontrollers, the different control loops have changed from analog to digital implementation, which allows more advanced control features. However, problems are still raised when designing high-performance current loop [miller,1990].

The main idea of current control method is timing and width of the voltage pulses. Two methods are too used in the current control, one is voltage chopping control method, and the other is hysteresis control method.

2.2.1 Voltage chopping control method

The voltage chopping control method compares a control signal $V_{control}$ (constant or slowly varying in time) with a repetitive switching-frequency triangular waveform or Pulse Width Modulation (PWM) in order to generate the switching signals. Controlling the switch duty ratios in this way allowed the average dc voltage output to be controlled. In order to have a fast built-up of the excitation current, high switching voltage is required. Fig. 43 shows an asymmetric bridge converter for SR drive. The asymmetric bridge converter is very popular for SR drives, consists of two power switches and two diodes per phase. This type of the SR drive can support independent control of each phase and handle phase overlap. The asymmetric converter has three modes, which are defined as magnetization mode, freewheeling mode, and demagnetization mode as shown in Fig. 44.

Fig. 43. Asymmetric bridge converter for SR drive

(a) Magnetization   (b) Freewheeling   (c) Demagnetization
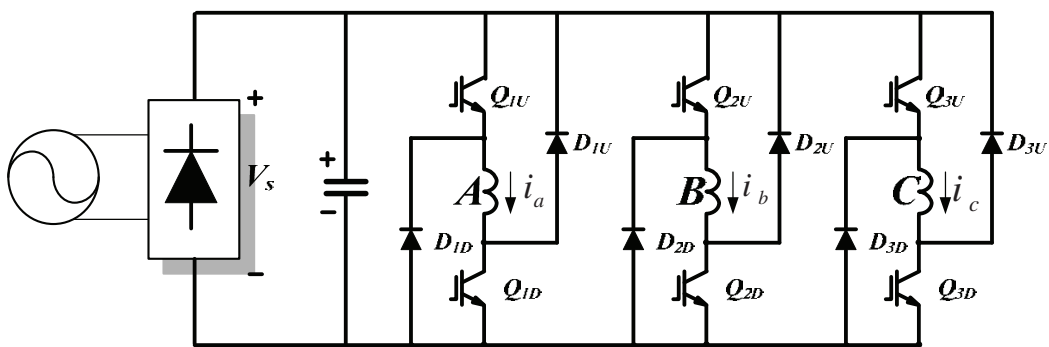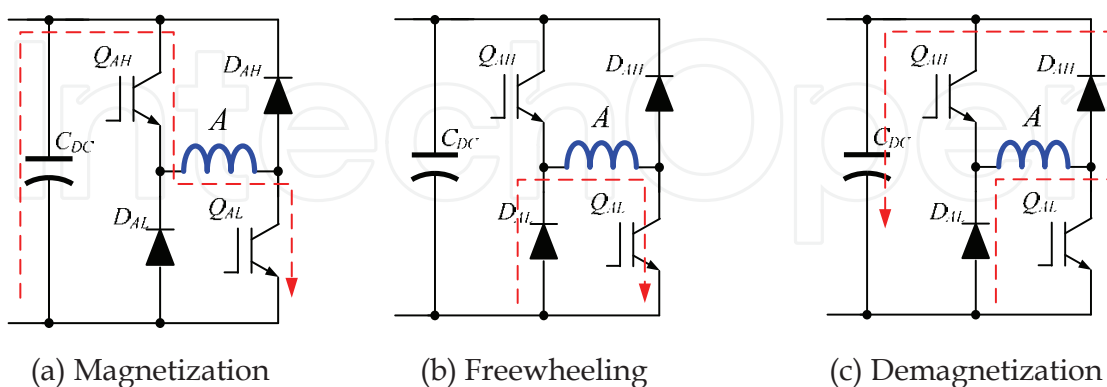
Fig. 44. Operation modes of asymmetric converter

From Fig. 44 (a) and (c), it is clear that amplitudes of the excitation and demagnetization voltage are close to terminal voltage of the filter capacitor. The fixed DC-link voltage limits the performance of the SR drive in the high speed application. On the other hand, the

voltage chopping method is useful for controlling the current at low speeds. This PWM strategy works with a fixed chopping frequency. The chopping voltage method can be separated into two modes: the hard chopping and the soft chopping method. In the hard chopping method both phase transistors are driven by the same pulsed signal: the two transistors are switched on and switched off at the same time. The power electronics board is then easier to design and is relatively cheap as it handles only three pulsed signals. A disadvantage of the hard chopping operation is that it increases the current ripple by a large factor. The soft chopping strategy allows not only control of the current but a minimization of the current ripple as well. In this soft chopping mode the low side transistor is left on during the dwell angle and the high side transistor switches according to the pulsed signal. In this case, the power electronics board has to handle six PWM signals [Liang,2006].

2.2.2 Hysteresis control method

Due to the hysteresis control, the current is flat, but if boost voltage is applied, the switching is higher than in the conventional case. The voltage of the boost capacitor is higher in the two capacitor parallel connected converter. The hysteresis control schemes for outgoing and incoming phases are shown on the right side of Fig. 45.

Solid and dash lines denote the rising and falling rules, respectively. The y axis denotes phase state and the x axis denotes torque error (ΔT_{err}), which is defined as,

$$\Delta T_{err} = T_{ref} - T_{est} \tag{35}$$

The threshold values of torque error are used to control state variation in hysteresis controller. Compared to previous research, this method only has 3 threshold values (ΔE, 0 and $-\Delta E$), which simplifies the control scheme. In order to reduce switching frequency, only one switch opens or closes at a time. In region 1, the incoming phase must remain in state 1 to build up phase current, and outgoing phase state changes to maintain constant torque. For example, assume that the starting point is (-1, 1), and the torque error is greater than 0. The switching states for the two phases will change to (0, 1). At the next evaluation period, the switching state will change to (1, 1) if torque error is more than ΔE and (-1, 1) if torque error is less than $-\Delta E$. So the combinatorial states of (-1, 1), (0, 0) and (1, 1) are selected by the control scheme. The control schemes for region 2 and region 3 are shown in Fig. 45(b) and (c), respectively.

3. Advanced torque control strategy

There are some various strategies of torque control: one method is direct torque control, which uses the simple control scheme and the torque hysteresis controller to reduce the torque ripple. Based on a simple algorithm, the short control period can be used to improve control precision. The direct instantaneous torque control (DITC) and advanced DITC (ADITC), torque sharing function (TSF) method are introduced in this section.

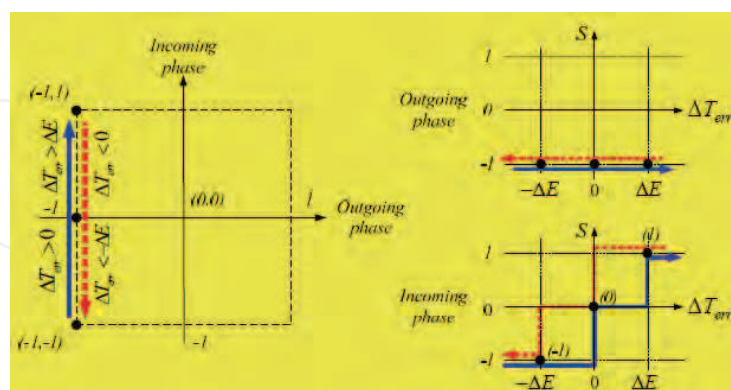### 3.1 Direct Instantaneous Torque Control (DITC)

The asymmetric converter is very popular in SRM drive system. The operating modes of asymmetric converter are shown in Fig. 46. The asymmetric converter has three states, which are defined as state 1, state 0 and state -1 in DITC method, respectively.
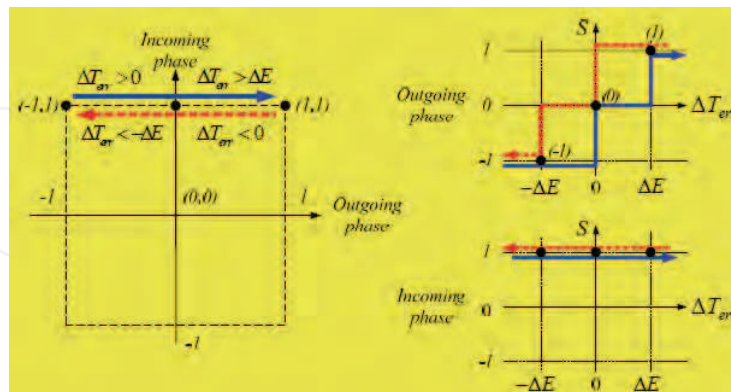
(a) Region 1
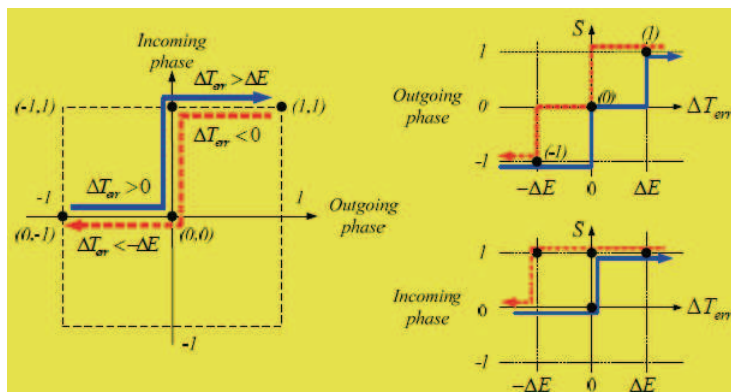
(b) Region 2

(c) Region 3

Fig. 45. The hysteresis control schemes for outgoing and incoming phases

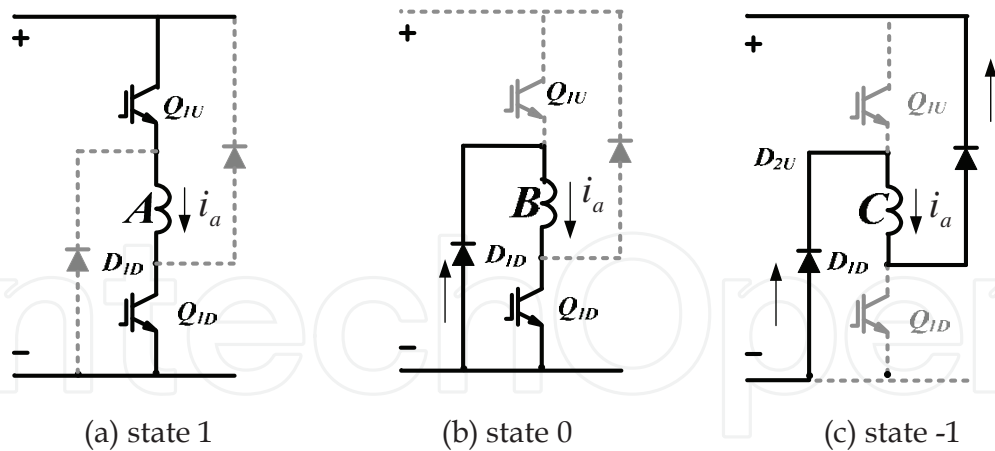(a) state 1   (b) state 0   (c) state -1

Fig. 46. 3 states in the asymmetric converter

In order to reduce a torque ripple, DITC method is introduced. By the given hysteresis control scheme, appropriate torque of each phase can be produced, and constant total torque can be obtained. The phase inductance has been divided into 3 regions shown as Fig. 47. The regions depend on the structure geometry and load. The boundaries of 3 regions are θ_{on1}, θ_1, θ_2 and θ_{on2} in Fig. 47. θ_{on1} and θ_{on2} are turn-on angle in the incoming phase and the next incoming phase, respectively, which depend on load and speed. The θ_1 is a rotor position which is initial overlap of stator and rotor. And θ_2 is aligned position of inductance in outgoing phase. Total length of these regions is 120 electrical degrees in 3 phases SRM. Here, let outgoing phase is phase A and incoming phase is phase B in Fig. 47. When the first region 3 is over, outgoing phase will be replaced by phase B in next 3 regions.

The DITC schemes of asymmetric converter are shown in Fig. 48. The combinatorial states of outgoing and incoming phase are shown as a square mesh. x and y axis denote state of outgoing and incoming phase, respectively. Each phase has 3 states, so the square mesh has 9 combinatorial states. However, only the black points are used in DITC scheme.
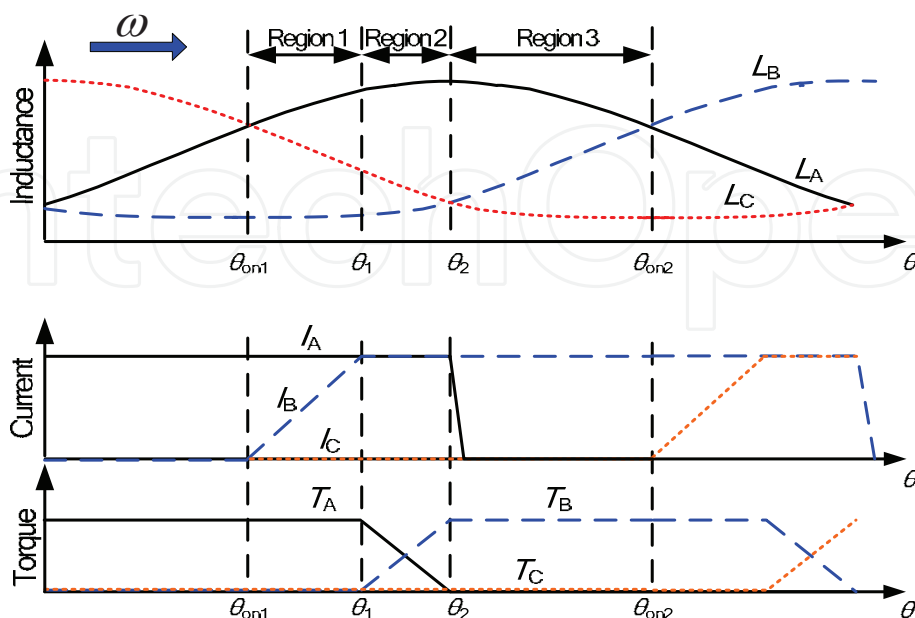
Fig. 47. Three regions of phase inductance in DITC method

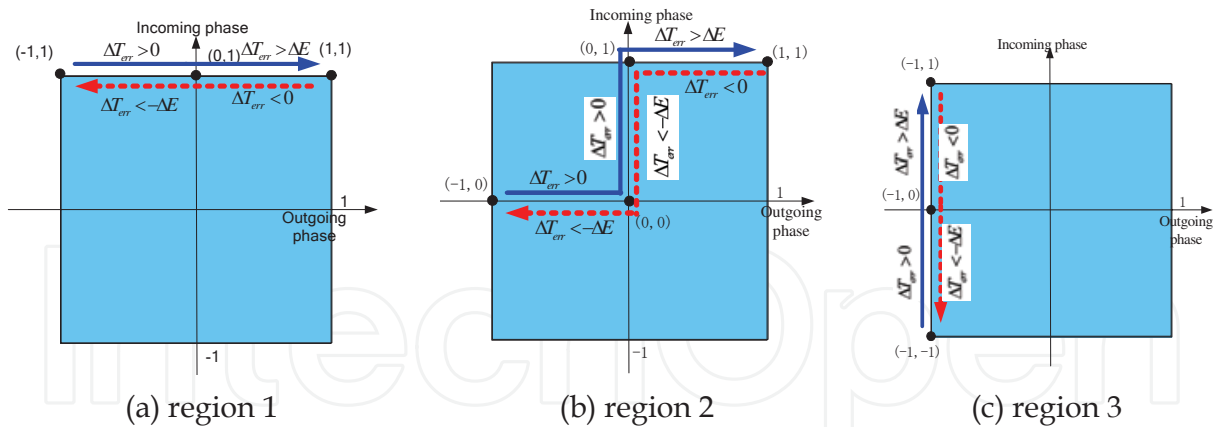(a) region 1   (b) region 2   (c) region 3

Fig. 48. DITC scheme of asymmetric converter

Control diagram of DITC SR motor drive is shown in Fig. 49. The torque estimation block is generally implemented by 3-D lookup table according to the phase currents and rotor position. And the digital torque hysteresis controller which carries out DITC scheme generates the state signals for all activated machine phases according to torque error between the reference torque and estimated torque. The state signal is converted as switching signals by switching table block to control converter.

Through estimation of instantaneous torque and a simple hysteresis control, the average of total torque can be kept in a bandwidth. And the major benefits of this control method are its high robustness and fast toque response. The switching of power switches can be reduced.

However, based on its typical hysteresis control strategy, switching frequency is not constant. At the same time, the instantaneous torque cannot be controlled within a given bandwidth of hysteresis controller. The torque ripple is limited by the controller sampling time, so torque ripple will increase with speed increased.
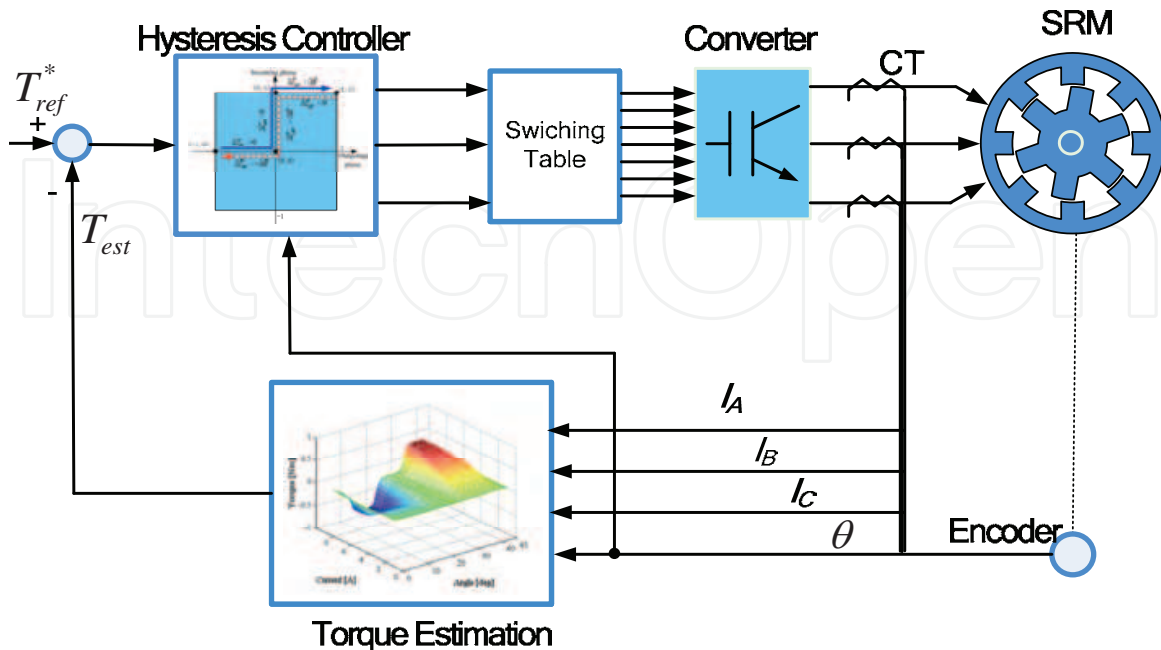
Fig. 49. Control diagram of DITC

3.2 Advanced Direct Instantaneous Torque Control (ADITC)

The conventional DITC method uses a simple hysteresis switch rules, so only one phase state is applied according to torque error at every sampling period. The toque variation with sampling time and speed under full dc-link voltage is shown in Fig. 50. In order to guarantee the torque ripple within a range, it has two methods: one is that reduces sampling time, which will increase the cost of hardware. Another is that control average voltage of phase winding in sampling time. PWM method can be used.
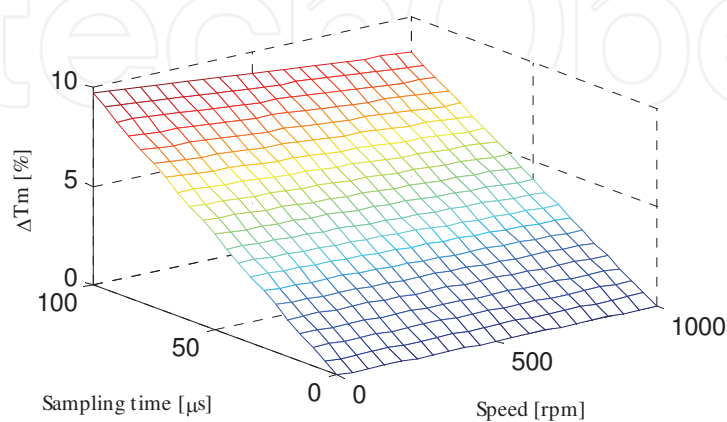
Fig. 50. Torque variation with sampling time and speed

ADITC combines the conventional DITC and PWM method. The duty ratio of the phase switch is regulated according to the torque error and simple control rules of DITC. Therefore, the sampling time of control can be extended, which allows implementation on low cost microcontrollers.

ADITC is improved from the conventional DITC, so the divided region of phase inductance is similar to DITC method. The control scheme of ADITC is shown in Fig. 51, $D_{t(k)}$ means incoming phase, $D_{t(k-1)}$ means outgoing phase. X-axis denotes torque error, and y-axis denotes switching state of $D_{t(k)}$ and $D_{t(k-1)}$.

(a) Region 1   (b) Region 2   (c) Region
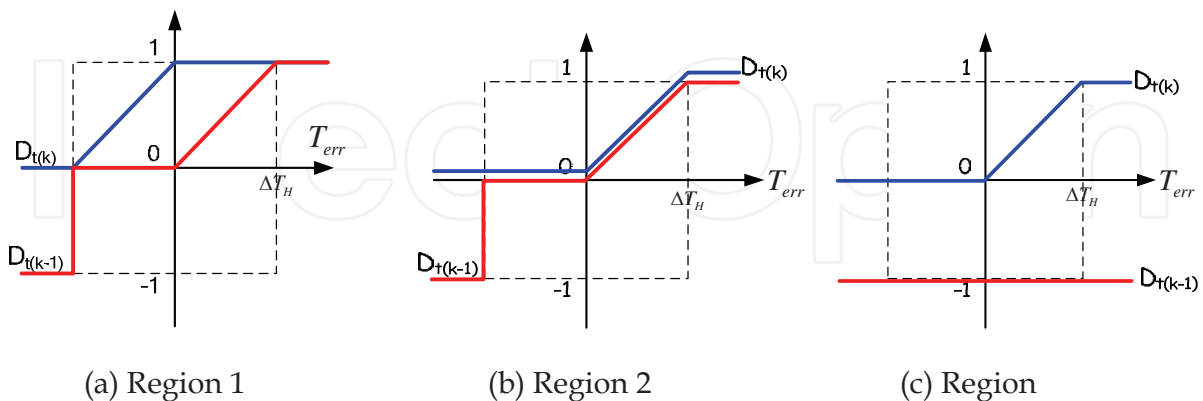
Fig. 51. ADITC scheme of asymmetric converter

Profit from the effect of PWM, the average voltage of phase winding can be adjusted from 0 to V_{dc} in one sampling time. And the hysteresis rule is removed from the control scheme. Now, the current state can select the phase state between state 0 and 1 by duty ratio of PWM.

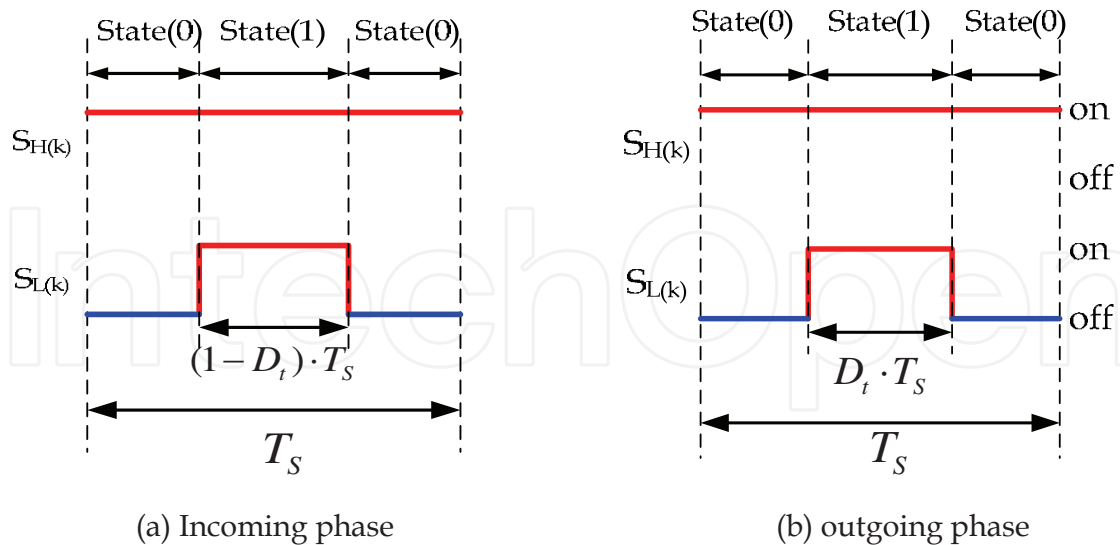(a) Incoming phase   (b) outgoing phase

Fig. 52. Switching modes of incoming and outgoing phase

The duty ratio of switching modes is decided by the torque error as shown in Fig. 52, and D_t is expressed as follows:

$$D_t = Abs\ (T_{err})/\Delta T_H \tag{36}$$

Where, T_{err} is torque error, ΔT_H is torque error bandwidth. The control block diagram of ADITC is similar to Fig. 53. The hysteresis controller is replaced by Advanced DITC controller, and the PWM generator is added.
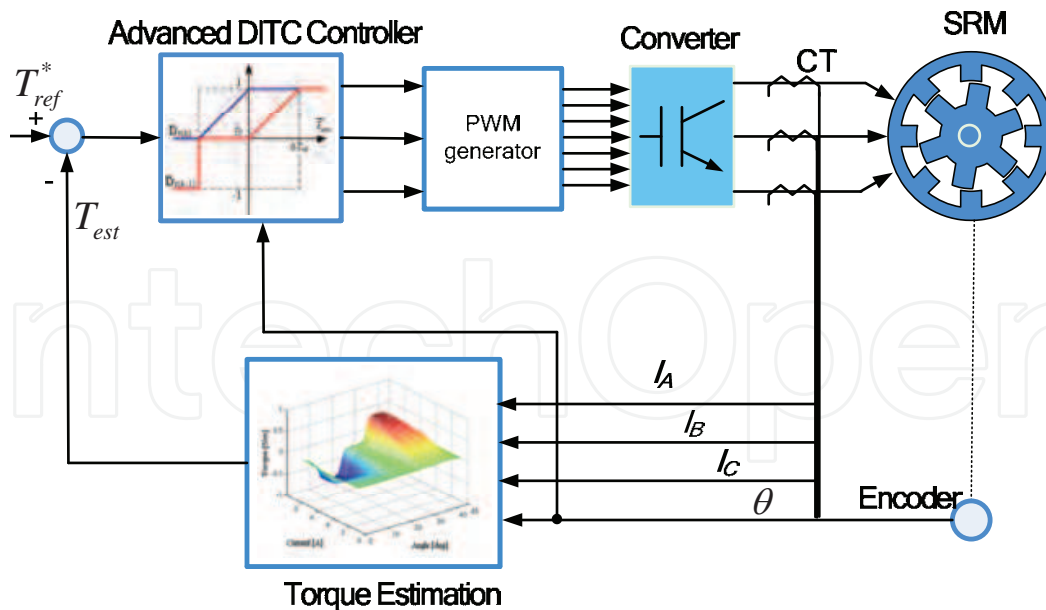
Fig. 53. Control diagram of ADITC

ADITC method can adjust average phase voltage to control variety of phase current in one sampling time, which can extend the sampling time and obtain smaller torque ripple than conventional DITC. However, PWM generator is added, and the switching frequency of

ADITC is double of DITC's with uniform sampling time in the worst case. So the switching loss and EMC noise are increased in ADITC method.

3.3 Torque sharing control

Another control method to produce continuous and constant torque is indirect torque control, which uses the complicated algorithms or distribution function to distribute each phase torque and obtain current command. And then, the current controller is used to control phase torque by given current command. The linear, cosine and non linear logical torque sharing function (TSF) are introduced.

Among them, the simple but powerful method is torque sharing function (TSF). The TSF method uses the pre-measured non-linear torque characteristic, and simply divided torque sharing curve is used for constant torque generation. Besides the direct torque control method, another method is indirect torque control. TSF is simple but powerful and popular method among the indirect torque control method. It simply divided by torque sharing curve that is used for constant torque generation. And the phase torque can be assigned to each phase current to control smoothing torque. But phase torque has relationship of square current. So the current ripple should keep small enough to generate smooth torque. So the frequency of current controller should be increased.

Fig. 54 shows the torque control block diagram with TSF method. The input torque reference is divided into three-phase torque command according to rotor position. Torque references of each phase are changed to current command signal in the "Torque-to-Current" block according to rotor position. Since the output torque is determined by the inductance slope and phase current, and the inductance slope is changed by rotor position, so the reference currents of each phase is determined by the target torque and rotor position. The switching rule generates an active switching signal of asymmetric converter according to current error and hysteresis switching tables.
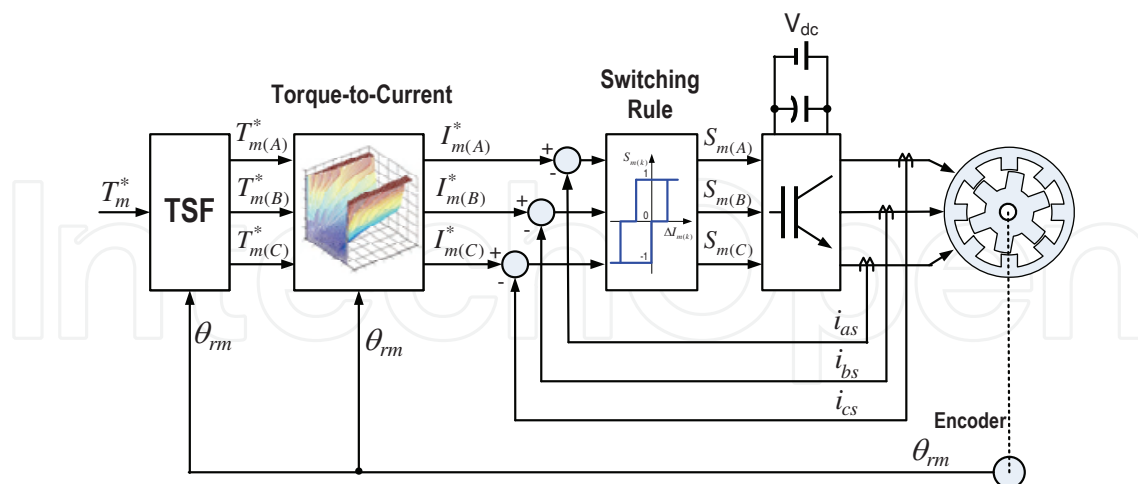

Fig. 54. The torque control block diagram with TSF method

In the over-lap region of inductances, the two-phase currents generate the output torque together. A simple torque sharing curves are studied for constant torque generation in the commutation region such as linear and cosine function.

Fig. 55 shows the inductance profiles of three-phase SRM, cosine and linear TSF curves. As shown in Fig. 55, region 2 denotes the one phase activation area. Region 1 and region 3 are

two phases activation area explained as the commutation region. In one phase activation region, TSF is constant in every torque sharing functions. But TSF is different in the commutation regions. The linear TSF has constant slope of torque in commutation region. This method is simple, but it is very difficult to generate the linear torque slope in the commutation region due to the non-linear inductance characteristics.
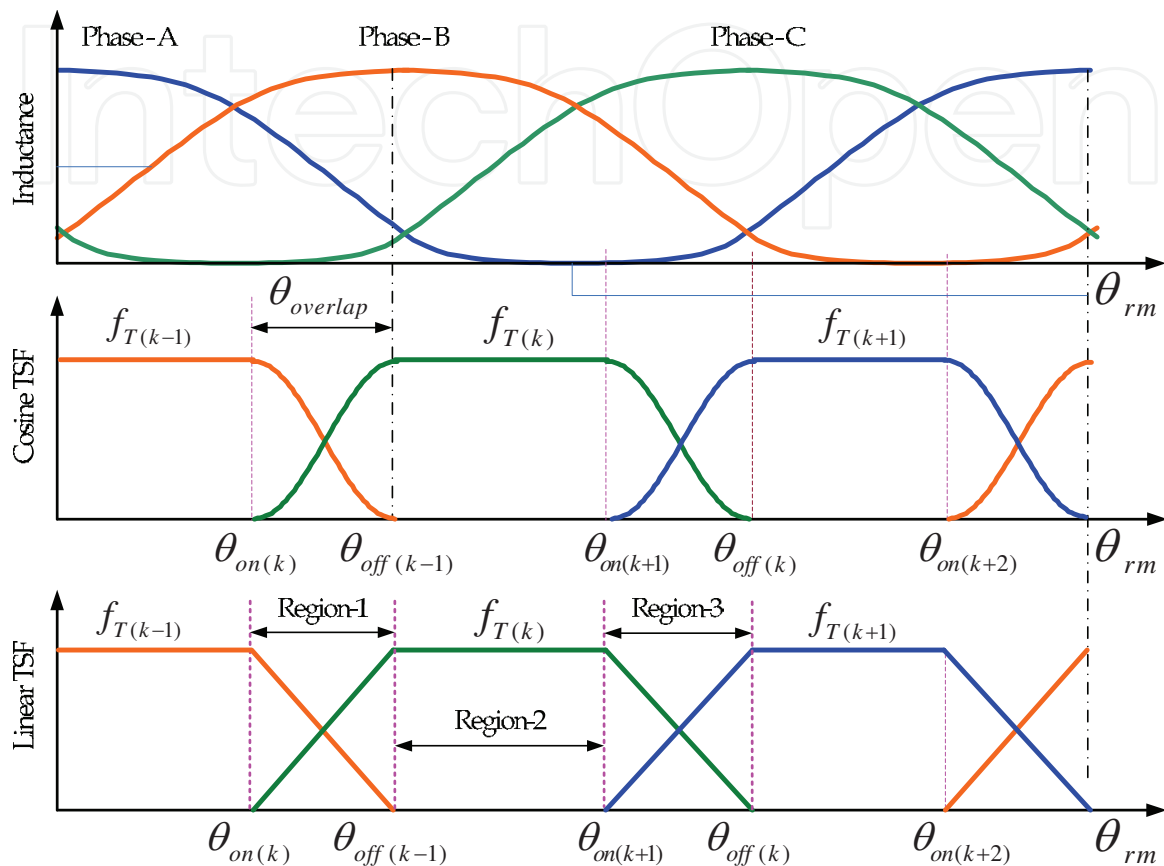

Fig. 55. Phase inductances and cosine, and linear TSF curves

The cosine TSF uses the cosine function in commutation region as shown in Fig. 55. The cosine function is relatively simple and it is similar to the non-linear inductance characteristics. But the non-linear characteristic of SRM is very complex, so cosine torque function can not be satisfied in the aspect of torque ripple and efficiency.

In the cosine TSF, the TSF of each phase in the commutation region are defined as follow

$$f_{T(k)} = \frac{1}{2}\left[1 - \cos\left(\frac{\theta_{rm} - \theta_{on(k)}}{\theta_{overlap}}\pi\right)\right] \tag{37}$$

$$f_{T(k-1)} = 1 - f_{T(k)} \tag{38}$$

$$f_{T(k+1)} = 0 \tag{39}$$

And the linear TSF method, the TSF of each phase can be obtained as follow

$$f_{T(k)} = \frac{\theta_{rm} - \theta_{on(k)}}{\theta_{overlap}} \tag{40}$$

$$f_{T(k-1)} = 1 - f_{T(k)} \tag{41}$$

$$f_{T(k+1)} = 0 \tag{42}$$

These two TSFs are very simple, but they can not consider nonlinear phenomena of the SRM and torque dip is much serious according to rotor speed. For the high performance torque control, a novel non-linear torque sharing function is suitable to use. In order to reduce torque ripple and to improve efficiency in commutation region, the TSF uses a non-linear current distribution technique at every rotor position. And the torque sharing function can be easily obtained by the current coordinates of each rotor position. In the commutation region, the total torque reference is divided by two-phase torque reference.

$$T_m^* = T_{m(k)}^* + T_{m\,(k+1)}^* \tag{43}$$

In the equation, the subscripts *k+1* denotes the incoming phase and k denotes outgoing phase. The actual torque can be obtained by inductance slope and phase current. So the torque equation can be derived as follows.

$$T_m^* = \frac{I_{m(k)}^{*\,2}}{a^2} + \frac{I_{m(k+1)}^{*\,2}}{b^2} \tag{44}$$

where,
$$a = \sqrt{\frac{2}{\partial L_{(k)}/\partial L_{(m)}}}, \quad b = \sqrt{\frac{2}{\partial L_{(k+1)}/\partial L_{(m)}}} \tag{45}$$

This equation is same as ellipse equation. In order to generate a constant torque reference, current references of the outgoing and incoming phases is placed on the ellipse trajectory in the commutation region. And the aspect of the ellipse and its trajectory is changed according to rotor position, inductance shape and the reference torque. Since the TSFs uses a fixed torque curve such as linear and cosine, the outgoing phase current should keep up the reference. And the actual current should remain higher level around rotor aligned position. Fig. 56 shows each phase current reference and actual phase torque for constant torque production according to rotor position. As shown in Fig. 56, the actual torque profile has non-linear characteristics around match position of rotor and stator position. So the current reference of each phase for constant torque generation is changed according to the rotor position and the amplitude of the torque reference. However, the actual phase current is limited by the performance of a motor and a drive. And the actual torque can not be satisfied the torque reference around the aligned position due to the non-linear torque characteristics shown as Fig. 56. If the current of outgoing phase is increased as a limit value of the motor, the actual torque is decreased after D_k position. And the actual torque of incoming phase can not be satisfied at the start position of the commutation due to the same reason. In order to generate the constant torque from A_k to G_{k+1}, the outgoing and incoming current reference should be properly selected so that the total torque of each phase is remained as constant value of T_m^*.

In order to reduce the commutation region, the outgoing phase current should be decreased fast, and the incoming phase current should be increased fast with a constant torque generation. At the starting point of commutation, the incoming phase current should be increased from zero to A_{k+1} point, and the end of the commutation, the outgoing phase current should be decreased from G_k point to zero as soon as possible shown in Fig. 56.
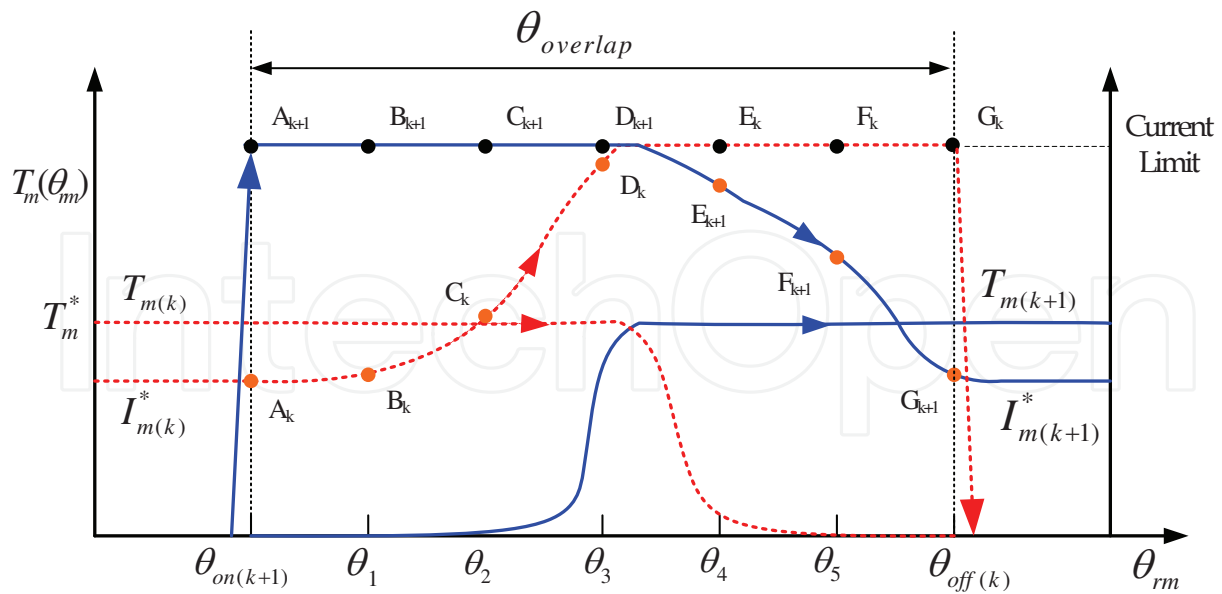
Fig. 56. Phase current and actual torque trajectory for constant torque production during phase commutation

In order to reduce the torque ripple and increase the operating efficiency, a non-linear TSF is based on minimum changing method. One phase current reference is fixed, and the other phase current reference is changed to generate constant torque during commutation. Fig. 57 shows the basic principle of the non-linear TSF commutation method.
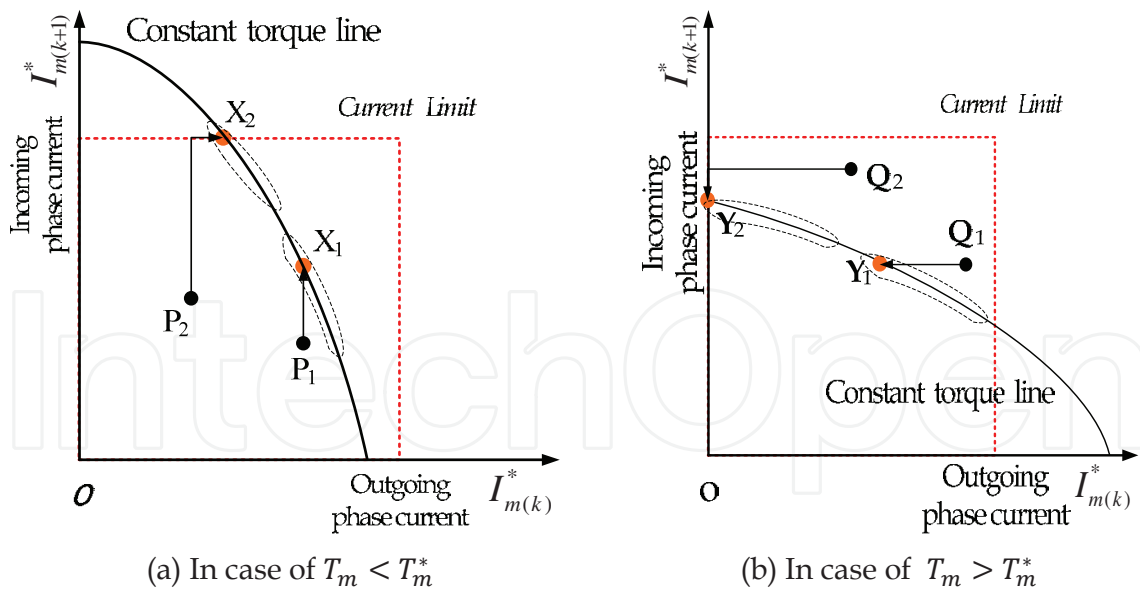

(a) In case of $T_m < T_m^*$ (b) In case of $T_m > T_m^*$

Fig. 57. Basic principle of the commutation method based on minimum changing

In this method, the incoming phase current is changed to a remaining or an increasing direction to produce the primary torque. And the outgoing phase current is changed to a remaining or a decreasing direction to produce the auxiliary torque. In case of $T_m < T_m^*$, the outgoing phase current is fixed, and the incoming phase current is increased to reach the constant torque line from P_1 to X_1 shown as Fig. 57(a). If the incoming phase current is

limited by the current limit and the actual torque is under the reference value, the auxiliary torque is generated by the outgoing phase current from P_2 to X_2 shown as Fig. 57(a). In case of $T_m > T_m^*$, the incoming phase current is fixed, and the outgoing phase current is decreased to reach the constant torque line from Q_1 to Y_1 shown as Fig. 57(b), because the incoming phase current is sufficient to generate the reference torque. If the outgoing phase current is reached to zero, and the actual torque is over to reference value, the incoming phase current is decreased from Q_2 to Y_2 shown as Fig. 57(b). This method is very simple, but the switching number for torque control can be reduced due to the minimum number changing of phase. As the other phase is fixed as the previous state, the torque ripple is dominated by the one phase switching. Especially, the outgoing phase current is naturally decreased when the incoming phase current is sufficient to produce the torque reference. The demagnetization can be decreased fast, and the tail current which generates negative torque can be suppressed.

Table 6 shows the logical TSF, and the Fig. 58 is the ideal current trajectory during commutation region. In Fig. 58, the ellipse curves are current trajectory for constant torque at each rotor position under commutation.

In case of $T_m < T_m^*$		when		In case of $T_m > T_m^*$	when
$T_{m(k+1)}^*$	$T_m^* - T_{m(k)}$	$I_{m(k+1)}^* < I_{max}$	$T_{m(k)}^*$	$T_m^* - T_{m(k+1)}$	$I_{m(k)}^* > 0$
	$T_{m\,(k+1)*}$ *At current limit*	$I_{m(k+1)}^* > I_{max}$		0	$I_{m(k)}^* < 0$
$T_{m(k)}^*$	$T_m^* - T_{m(k+1)}^*$		$T_{m(k+1)}^*$	$T_{m(k+1)}$	$I_{m(k)}^* > 0$
				$T_m^* - T_{m(k)}$	$I_{m(k)}^* < 0$

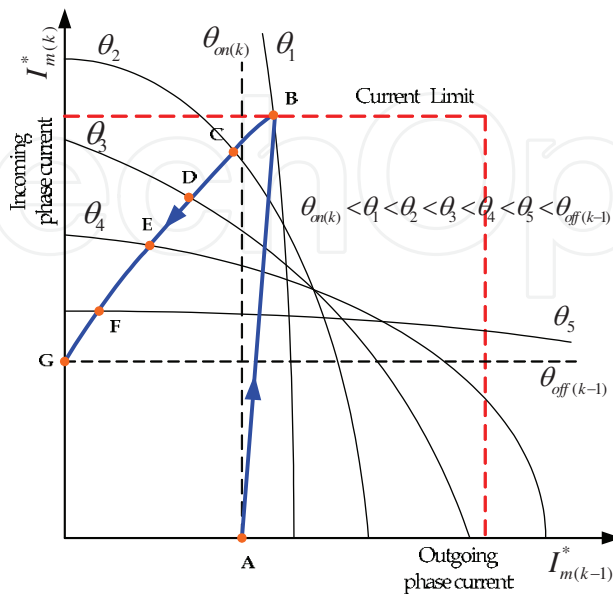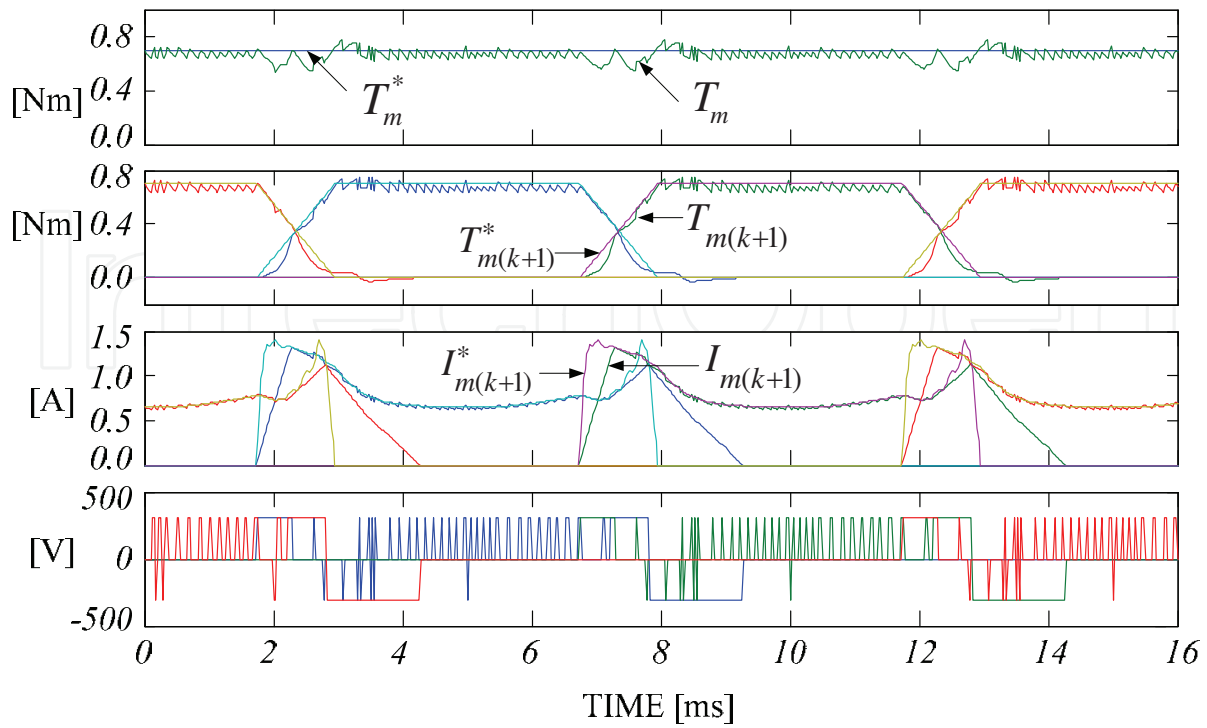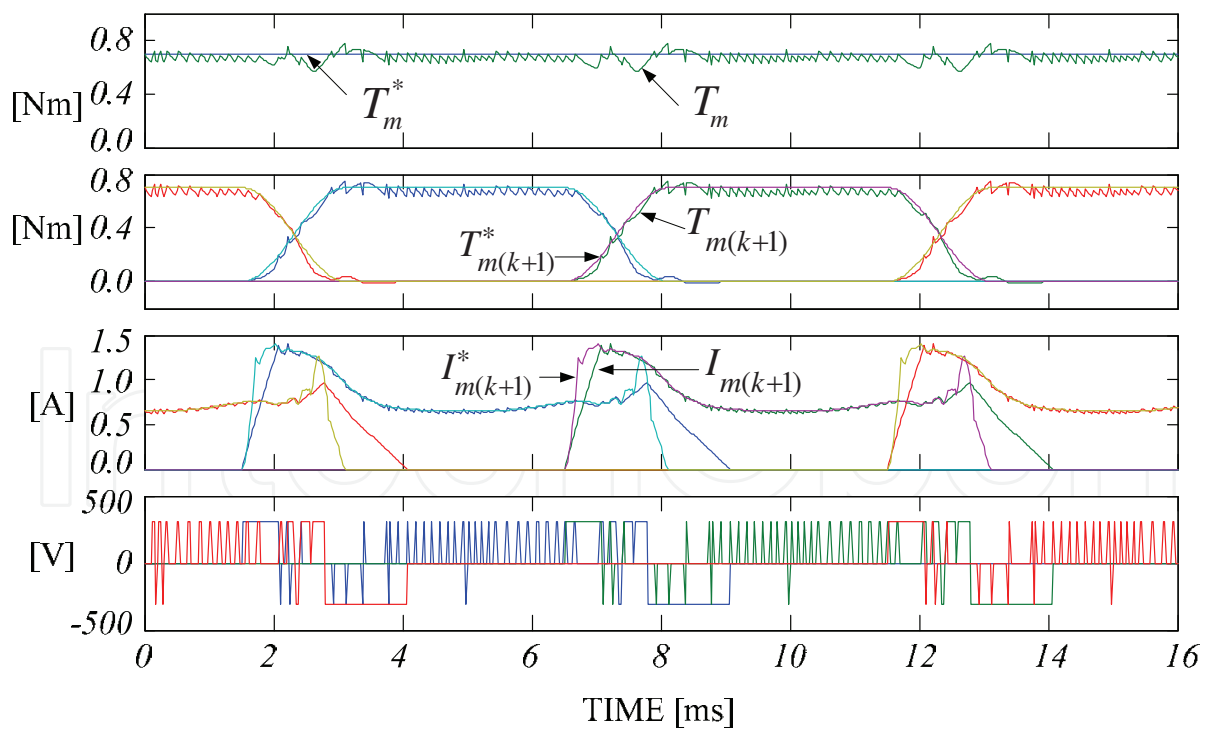Table 6. The logical TSF in commutation region.

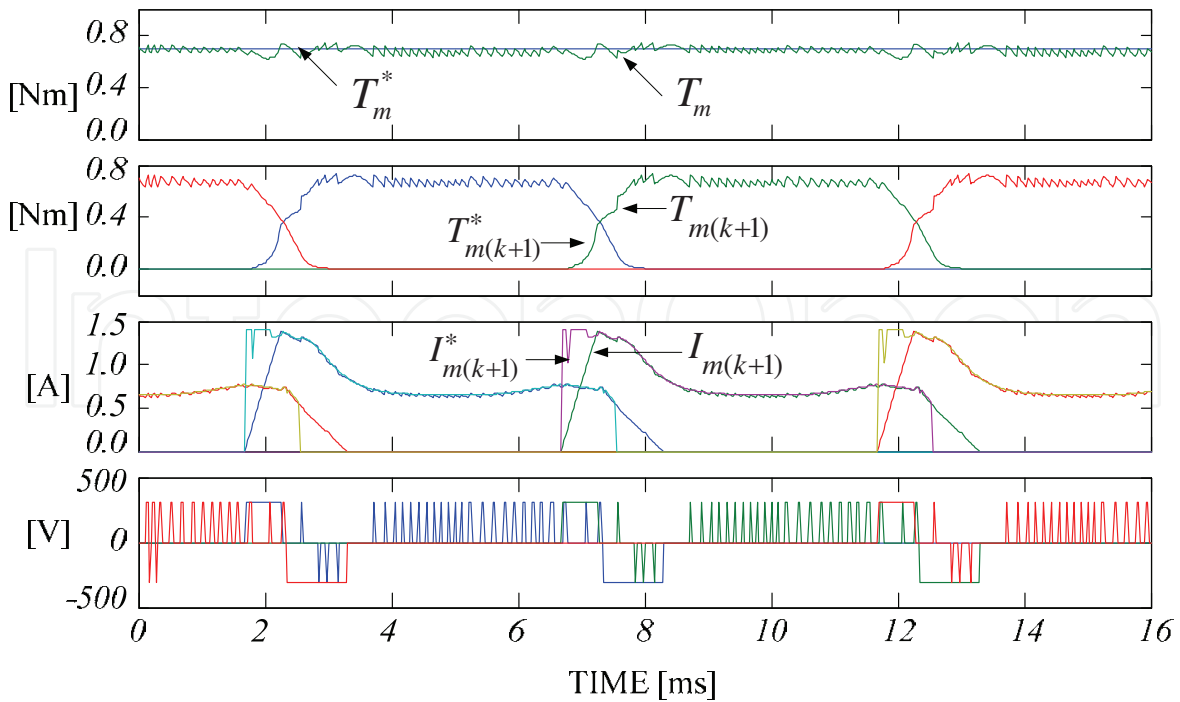Fig. 58. The ideal current trajectory at commutation region

(a) Linear TSF

(b) Cosine TSF

Fig. 59. Simulation result at 500 rpm with rated torque

(c) non-linear Logical TSF

Fig. 59. Simulation results at 500rpm with rated torque (continued)

In order to verify the non-linear TSF control scheme, computer simulations are executed and compared with conventional methods. Matlab and simulink are used for simulation. Fig. 59 shows the simulation comparison results at 500[rpm] with rated torque reference. The simulation results show the total reference torque, actual total torque, reference phase torque, actual phase torque, reference phase current, actual phase current and phase voltage, respectively. As shown in Fig. 59, torque ripple is linear TSF > cosine TSF > the logical TSF.

Fig. 60 shows the actual current trajectory in the commutation region. In the conventional case, the cross over of the outgoing and incoming phase is serious and two-phase current are changed at each rotor position. But the cross over is very small and one-phase current is changed at each rotor position in the logical TSF method.

(a) Linear TSF   (b) Cosine TSF   (c) logical TSF
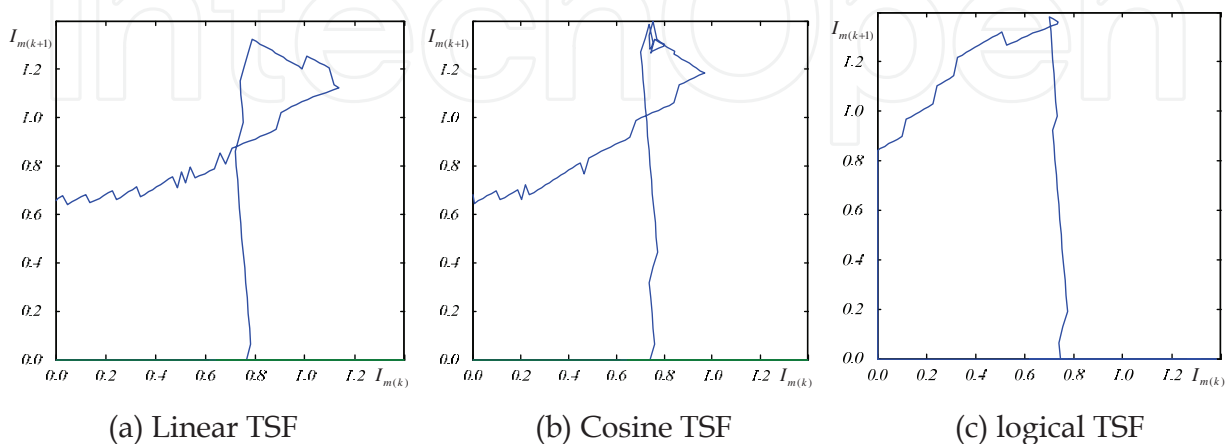
Fig. 60. The current trajectory for constant torque production in commutation region

Fig. 61 shows the experimental setup. The main controller is designed by TMS320F2812 from TI(Texas Instruments) and phase current and voltage signals are feedback to 12bit ADC embedded by DSP. The rotor position and speed is obtained by 512ppr optical encoder. At every 1.6[ms], the rotor speed is calculated from captured encoder pulse by QEP function of DSP.
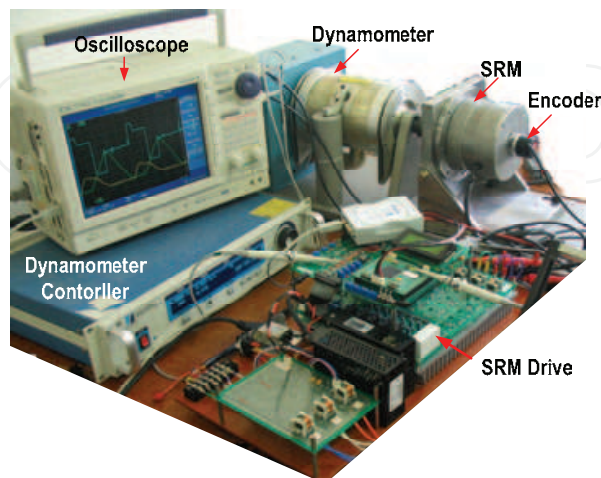

Fig. 61. The experimental configuration

Fig. 62, 63 and 64 show the experimental results in case of linear TSF, cosine TSF and the non-linear logical TSF at 500rpm, respectively. Torque ripple can be reduced in case of the TSF method due to the minimum phase changing.

(a)   (b)
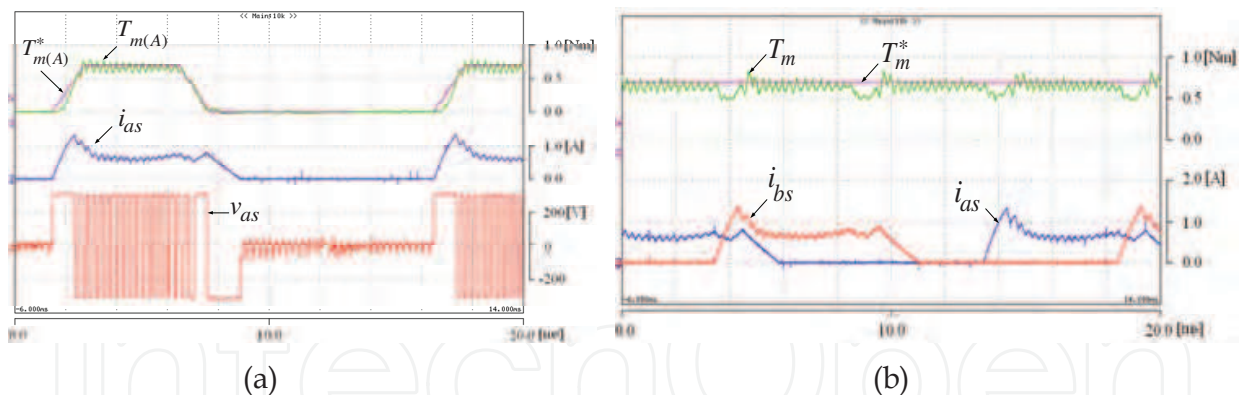
Fig. 62. Experimental results in linear TSF(at 500[rpm])
(a) Reference torque, actual torque, phase current and terminal voltage
(b) Total reference torque, actual torque and phase currents

Fig. 65 shows experimental results at 1200rpm. As speed increase, torque ripple is increased due to the reduction of the commutation time. However, the control performance is much improved in this case.

Fig. 66 shows efficiency of the logical control schemes. In the low speed range, the TSF control scheme has about 5% higher efficiency than that of the conventional ones with low torque ripple. In high speed range, the actual efficiency is similar to all other control method due to the short commutation time. But the practical torque ripple can be reduced than other two control schemes shown in simulation and experimental results.
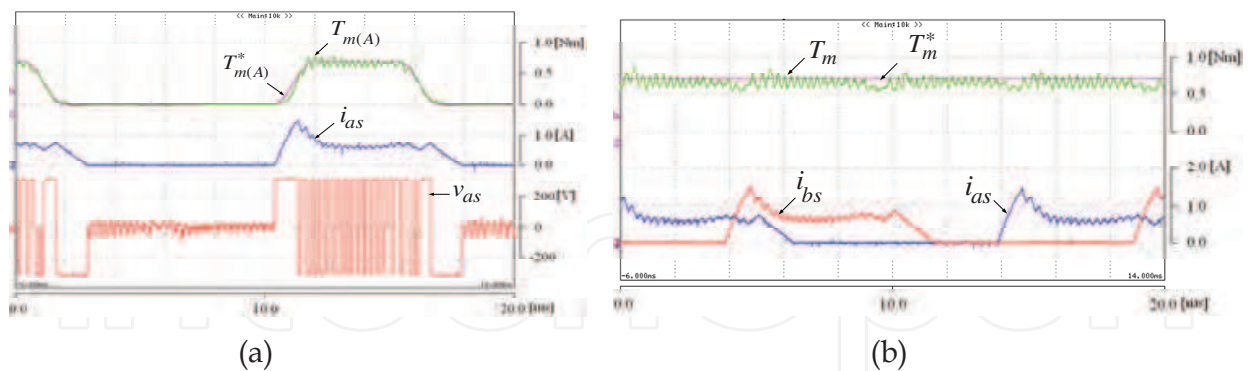
Fig. 63. Experimental results in cosine TSF(at 500[rpm])
(a) Reference, actual torque, phase current and terminal voltage
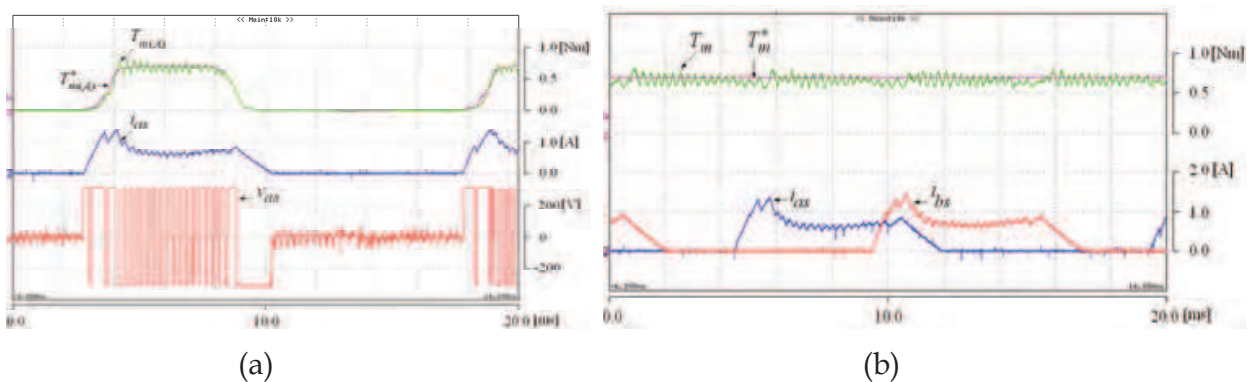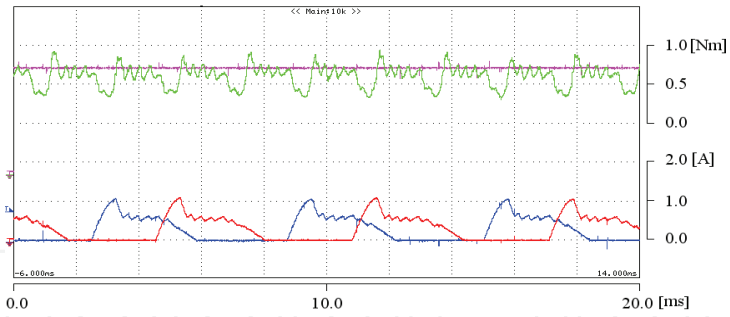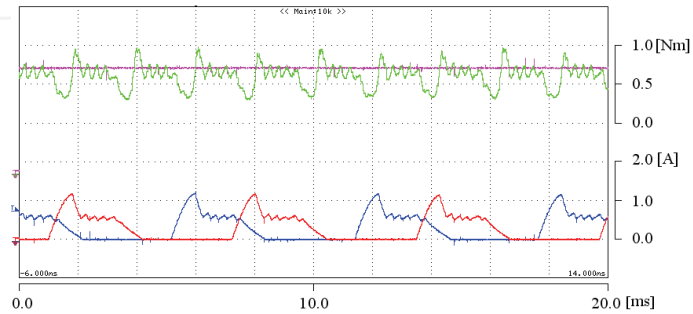(b) Total reference torque, actual torque and phase currents

Fig. 64. Experimental results in case of the non-linear logical TSF(at 500[rpm])
(a) Reference, actual torque, phase current and terminal voltage
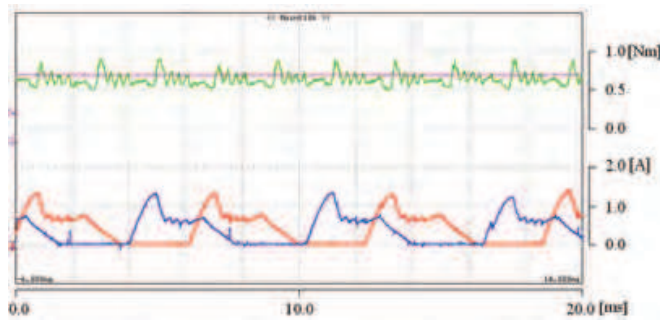(b) Total reference torque, actual torque and phase currents

4. Conclusion

The torque production in switched reluctance motor structures comes from the tendency of the rotor poles to align with the excited stator poles. However, because SRM has doubly salient poles and non-linear magnetic characteristics, the torque ripple is more severe than these of other traditional motors. The torque ripple can be minimized through magnetic circuit design or drive control. By controlling the torque of the SRM, low torque ripple, noise reduction or even increasing of the efficiency can be achieved. There are many different types of control methods. In this chapter, detailed characteristics of each control method are introduced in order to give the advanced knowledge about torque control method in SRM drive.

(a) Reference torque, total torque and phase currents in linear TSF

(b) Reference torque, total torque and phase currents in cosine TSF

(c) Reference torque, total torque and phase currents in non-linear logical TSF

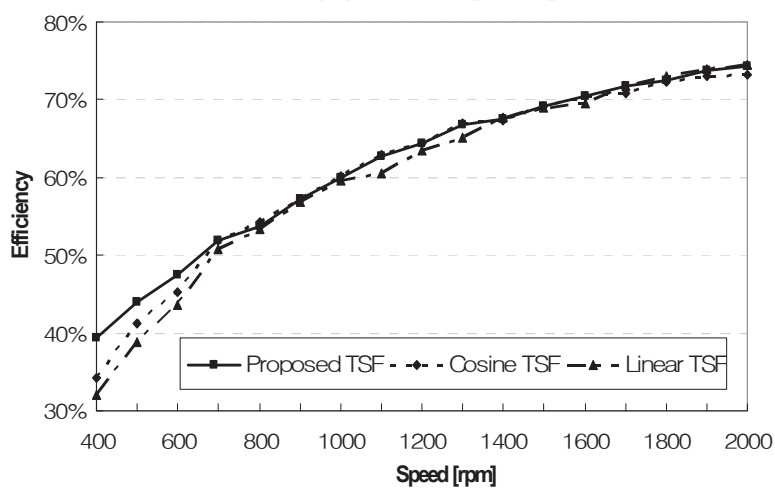Fig. 65. Experimental results at 1200rpm with rated torque

Fig. 66. Efficiency comparison

5. References

A. Chiba, K. Chida and T. Fukao, "Principles and Characteristics of a Reluctance Motor with Windings of Magnetic Bearing," in *Proc. PEC Tokyo*, pp.919-926, 1990.

Bass, J. T., Ehsani, M. and Miller, T. J. E ; "Robust torque control of a switched reluctance motor without a shaft position sensor," *IEEE Transactions*, Vol.IE-33, No.33, 1986, 212-216.

Bausch, H. and Rieke, B.; "Speed and torque control of thyristorfed reluctance motors." *Proceedings ICEM*, Vienna Pt.I, 1978, 128.1-128.10. Also : "Performance of thyristorfed electric car reluctance machines." *Proceedings ICEM*, Brussels E4/2.1-2.10

Byrne, J. V. and Lacy, J.G.; "Characteristics of saturable stepper and reluctance motors." *IEE Conf.* Publ. No.136,Small Electrical Machines, 1976, 93-96.

Corda, J. and Stephenson, J. M., "Speed control of switched reluctance motors," *International Conference on Electrical Machines*, Budapest, 1982.

Cossar, C. and miller, T.J.E., "Electromagnetic testing of switched reluctance motors," *International Conference on Electrical Machines*, Manchester, September 15-17, 1992, 470-474.

Davis, R. M., "A Comparison of Switched Reluctance Rotor Structures," *IEEE Trans. Indu. Elec.*, Vol.35, No.4, pp.524-529, Nov. 1988.

D.H. Lee, J. Liang, Z.G. Lee, J.W. Ahn, "A Simple Nonlinear Logical Torque Sharing Function for Low-Torque Ripple SR Drive", Industrial Electronics, *IEEE Transactions* on, Vol. 56, Issue 8, pp.3021-3028, Aug. 2009.

D.H. Lee, J. Liang, T.H. Kim, J.W. Ahn, "Novel passive boost power converter for SR drive with high demagnetization voltage", International Conference on Electrical Machines and Systems, 2008, pp.3353-3357, 17-20 Oct. 2008.

D.H. Lee, T.H. Kim, J.W. Ahn, " Pressure control of SR Driven Hydraulic Oil-pump Using Data Based PID Controller", *Journal of Power Electronics* Vol.9, September 2009.

D.S. Schramm, B.W. Williams, and T.C. Green; "Torque ripple reduction of switched reluctance motors by phase current optimal profiling", in *Proc. IEEE PESC' 92*, Vol. 2, Toledo, Spain, pp.857-860, 1992 .

Harris, M. R. and Jahns, T. M., "A current-controlled switched reluctance drive for FHP applications," *Conference on Applied Motion Control*, Minneapolis, June 10-12 , 1986.

Ilic-Spong, M., Miller, T. J. E., MacMinn, S. R. and Thorp, J. S., "Instantaneous torque control of electric motor drives," *IEEE Transactions*, Vol.IA-22, 1987, 708-715.

J.W. Ahn, Se.G. Oh, J.W. Moon, Y.M. Hwang; "A three-phase switched reluctance motor with two-phase excitation", Industry Applications, *IEEE Transactions* on, Vol. 35, Issue 5, pp.1067-1075, Sept.-Oct. 1999.

J.W. Ahn, S. G. Oh, and Y. M. Hwang, "A Novel Control Scheme for Low Cost SRM Drive, " in *Proc. IEEE/ISIE '95*, July 1995, Athens, pp. 279-283.

J.W. Ahn, S.G. Oh, " DSP Based High Efficiency SR Drive with Precise Speed Control", *PESC '99, june 27*, Charleston, south Carolina.

J.W. Ahn, "Torque Control Strategy for High Performance SR Drive", *Journal of Electrical Engineering & Technology(JEET)*, Vol.3. No.4. 2008, pp.538-545.

J.W. Ahn , S. G. Oh, C. U. Kim, Y. M. Hwang, "Digital PLL Technique for Precise Speed Control for SR Drive," in *Proc. IEEE/PESC'99*, Jun./Jul. 1999, Charleston, pp.815-819

J.M. Stephenson; J. Corda, "Computation of Torque and Current in Doubly-Salient Reluctance Motors from Nonlinear Magnetization Data", *Proceedings IEE*, Vol. 126, pp.393-396, May 1979.

J. N.Liang, Z. G. Lee, D. H. Lee, J. W. Ahn, " DITC of SRM Drive System Using 4-Level Converter " , *Proceedings of ICEMS 2006*, Vol. 1, 21-23 Nov. 2006

J. N. Liang, S.H. Seok, D.H. Lee, J.W. Ahn, "Novel active boost power converter for SR drive" *International Conference on Electrical Machines and Systems*, 2008, pp.3347-3352, 17-20 Oct. 2008.

Lawrenson, P.J.et al; "Variable-speed switched reluctance motors." *Proceedings IEE*. Vol.127, Pt.B 253-265,1980.

M. Stiebler, G. Jie; "A low Voltage switched reluctance motor with experimentally optimized control", *Proceedings of ICEM '92*, Vol. 2, pp. 532-536, Sep. 1992.

Miller, T. J. E., Bower, P. G., Becerra, R. and Ehsani, M., "Four- quadrant brushless reluctance motor drive," *IEE Conference on Power Electronics and Variable Speed Drives*, London, 1988.

Pollock, C. and Willams, B. W.; "Power convertor circuit for switched reluctance motors with the minimum number of switches," *IEE Proceedings-B*, Vol.137, 1990, No.6.

R. Krishnan; "*Switched Reluctance Motor Drives: Modeling, Simulation, Analysis, Design, and Applications*", CRC Press, 2001

R. Orthmann, H.P. Schoner; "Turn-off angle control of switched reluctance motors for optimum torque output", *Proceedings of EPE '93*, Vol. 6, pp.20-55, 1993.

Stephenson, J.M. and El-Khazendar, M.A., "Saturation in doubly salient reluctance motors," *IEE Proceedings-B*, Vol.136, No.1, 1989, 50-58.

T. Skvarenina; "*The Power Electronics Handbook*", CRC Press, 2002

T.J.E. Miller, M. McGilp, "Nonlinear theory of the switched reluctance motor for rapid computer-aided design", *IEE Proceedings B (Electric Power Applications)*, Vol. 137, No. 6, pp.337-347, Nov. 1990.

Unnewehr, L. E. and Koch, W. H.; "An axial air-gap reluctance motor for variable-speed applications." *IEEE Transactions*, 1974, PAS-93, 367-376.

Vukosavic, S. and Stefanovic, V. R., "SRM inverter topologies : a comparative evaluation," *IEEE IAS Annual Meeting*, Conf. Record, Seattle, WA, 1990.

Wallace, R. S. and Taylor, D. G., "Low torque ripple switched reluctance motors for direct-drive robotics," *IEEE Transactions on Robotics and Automation*, Vol.7, No.6, 1991, 733-742.

Wallace, R. S. and Taylor, D. G., "A balanced commutator for switched reluctance motors to reduce torque ripple," *IEEE Transactions on Power Electronics*, October 1992.
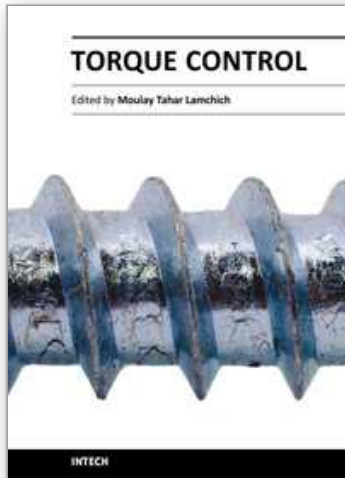
Torque Control

Edited by Prof. Moulay Tahar Lamchich

This book is the result of inspirations and contributions from many researchers, a collection of 9 works, which are, in majority, focalised around the Direct Torque Control and may be comprised of three sections: different techniques for the control of asynchronous motors and double feed or double star induction machines, oriented approach of recent developments relating to the control of the Permanent Magnet Synchronous Motors, and special controller design and torque control of switched reluctance machine.

How to reference

In order to correctly reference this scholarly work, feel free to copy and paste the following:

JIn-Woo Ahn (2011). Switched Reluctance Motor, Torque Control, Prof. Moulay Tahar Lamchich (Ed.), ISBN: 978-953-307-428-3, InTech, Available from: http://www.intechopen.com/books/torque-control/switched-reluctance-motor

INTECH
open science | open minds